

Melanie Hirz

Membrane Protein Expression

in *Pichia pastoris*

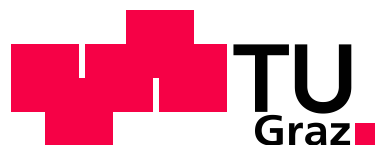
MASTERARBEIT

zur Erlangung des akademischen Grades eines
Diplom-Ingenieurs
der Studienrichtung Biotechnologie

eingereicht an der
Technischen Universität Graz

Ass. Prof. Dipl.-Ing. Dr. techn. Harald Pichler
Mag. Dr. Tamara Wriessnegger
Univ.-Prof. Dipl.-Ing. Dr. techn. Helmut Schwab

Institut für Molekulare Biotechnologie
Technische Universität Graz



Graz, 2012

Deutsche Fassung:
Beschluss der Curricula-Kommission für Bachelor-, Master- und Diplomstudien vom 10.11.2008
Genehmigung des Senates am 1.12.2008

EIDESSTÄTLICHE ERKLÄRUNG

Ich erkläre an Eides statt, dass ich die vorliegende Arbeit selbstständig verfasst, andere als die angegebenen Quellen/Hilfsmittel nicht benutzt, und die den benutzten Quellen wörtlich und inhaltlich entnommene Stellen als solche kenntlich gemacht habe.

Graz, am

.....
(Unterschrift)

Englische Fassung:

STATUTORY DECLARATION

I declare that I have authored this thesis independently, that I have not used other than the declared sources/resources, and that I have explicitly marked all material which has been quoted either literally or by content from the used sources.

.....
date

.....
(signature)

Danksagung

An erster Stelle möchte ich meinen Eltern und meinem Bruder dafür danken, dass sie immer an mich geglaubt und mich finanziell unterstützt haben. Ein großer Dank geht an Martin, der mir stets mit viel Toleranz und ermutigenden Worten zur Seite stand. Des Weiteren danke ich meinen Laborkollegen, die ich mittlerweile auch zu meinen engen Freunden zählen darf, für die vielen gemeinsamen lustigen Stunden beim Wandern, Eis machen, KUBB spielen und Filme schauen! Danke auch an meine Studienkollegen, die mir die gesamte Studienzzeit versüßt haben. Ohne sie hätte ich das Studium nicht in dieser Zeit und mit diesem Erfolg geschafft. Auch meinen Freunden außerhalb der Uni möchte ich herzlich danken, denn sie haben mir geholfen, den Kopf wieder einmal frei zu bekommen! Natürlich sei auch meinen lieben Betreuern, Tamara und Harald, für die ausgezeichnete Hilfestellung im Labor gedankt, ich konnte sehr viel von ihnen lernen. Sie haben einen großen Beitrag dazu geleistet, dass ich die Versuche erfolgreich durchführen konnte, und haben mir geholfen, etwaige Zweifel zu überwinden. Ich danke auch Erich Leitner für die Vermessung der GC-MS Proben und der Arbeitsgruppe von Günther Daum für die Bereitstellung von Antikörpern und die Einschulung für radioaktives Arbeiten. Zu guter Letzt danke ich Prof. Schwab, der bei den Seminaren stets hilfreiche Ratschläge geben konnte und die Diplomarbeit an diesem Institut schlussendlich ermöglicht hat.

Abstract

The human Na,K-ATPase is an important, integral membrane protein present in every cell of the human body. It interacts specifically with cholesterol and phospholipids, ensuring protein stability and enhancing ion transport activity. Due to the different membrane sterol composition in mammals and yeast, heterologous expression of membrane proteins is often impaired. Therefore, human Na,K-ATPase $\alpha 3\beta 1$ isoform was expressed and characterized in different *P. pastoris* strains producing other sterols than ergosterol. The focus of the work was mainly laid onto the cholesterol-producing *P. pastoris* strain. Western blot analyses revealed that the membrane protein formed by the cholesterol-producing yeast was more stable over time compared to other strains. ATPase activity assays suggested furthermore that the Na,K-ATPase was functionally expressed in the plasma membrane. Moreover, [^3H]-ouabain cell surface binding studies underscored that the Na,K-ATPase $\alpha 3\beta 1$ isoform was present in high numbers at the cell surface. This provides evidence that the humanized sterol composition positively influences Na,K-ATPase stability, activity and localization in the yeast plasma membrane. Prospectively, cholesterol-producing yeast will have high potential for functional expression of other Na,K-ATPase isoforms as well as many mammalian membrane proteins.

Zusammenfassung

Na,K-ATPasen sind integrale Membranproteine, deren Stabilität und Funktion durch die Interaktion mit Cholesterol und Phospholipiden gewährleistet wird. Die heterologe Expression dieser und vieler anderer Membranproteine in niederen Eukaryonten gestaltet sich jedoch schwierig, da die Plasmamembran von Hefen wie *P. pastoris* hauptsächlich Ergosterol und kein Cholesterol beinhaltet. Die Isoform $\alpha 3\beta 1$ der humanen Na,K-ATPase wurde daher in *P. pastoris* Stämmen, welche verschiedene Sterole produzieren, exprimiert und biochemisch charakterisiert. Besonderes Augenmerk wurde dabei auf den Cholesterol-produzierenden Stamm gelegt. Western Blot Experimente gaben erste Hinweise darauf, dass die $\alpha 3$ -Untereinheit der Na,K-ATPase stabiler exprimiert wird und das heterodimere Protein in der Plasmamembran lokalisiert ist. Na,K-ATPase Aktivitätstests zeigten weiters, dass das rekombinante Membranprotein eine höhere Aktivität als die Vergleichsstämme aufweist. Die Lokalisierung der Na,K-ATPase in der Plasmamembran und somit an der Zelloberfläche wurde mittels spezifischer Bindung des radioaktiv markierten Inhibitors [^3H]-Ouabain bestätigt. Diese Versuche zeigten, dass die Isoform $\alpha 3\beta 1$ der humanen Na,K-ATPase in einer Cholesterol-produzierenden Hefe stabiler exprimiert und zur Plasmamembran transportiert wird, wo sie eine höhere spezifische Aktivität aufweist. Dieser *P. pastoris* Stamm hat großes Potenzial für die Expression weiterer Isoformen der Na,K-ATPase, sowie auch anderer Membranproteine, die Interaktion mit Cholesterol für ihre Stabilität und Aktivität benötigen.

Table of Contents

Danksagung	3
Abstract	4
Zusammenfassung.....	5
List of abbreviations	8
1 Introduction	9
1.1 Role and function of Na,K-ATPases	9
1.2 Influence of lipids on Na,K-ATPase stability and activity	11
1.3 <i>P. pastoris</i> as expression host for human membrane proteins	12
1.4 Aim of this master thesis	13
2 Materials and Methods.....	14
2.1 Materials.....	14
2.1.1 Reagents.....	14
2.1.2 Media and buffers	16
2.1.3 Instruments and devices	19
2.1.4 Strains.....	20
2.1.5 Vectors.....	21
2.1.6 Primers	23
2.2 Methods.....	25
2.2.1 General methods.....	25
2.2.2 Construction of <i>P. pastoris</i> knockout and expression strains.....	28
2.2.3 Lipid analysis.....	31
2.2.4 Protein expression in <i>P. pastoris</i>	34
2.2.5 Activity assays.....	38
2.2.6 Radioligand binding studies	41
2.2.7 Immunofluorescence	45
3 Results.....	47
3.1 Growth studies of different <i>P. pastoris</i> strains	47

3.2	Construction of a <i>P. pastoris</i> $\Delta cho1$ knockout strain	48
3.2.1	Overlap extension PCR and sequencing of the <i>CHO1</i> knockout cassette.....	48
3.2.2	Transformation of <i>P. pastoris</i> WT and cPCR verification	49
3.2.3	Thin layer chromatography	50
3.3	Heterologous expression of Na,K-ATPase in different <i>P. pastoris</i> strains.....	51
3.3.1	Transformation of electrocompetent <i>P. pastoris</i> cells with pAO815- $\alpha 3\beta 1$	51
3.3.2	Colony PCR verification	51
3.3.3	Cell harvest and protein quantification	53
3.4	Western blot analysis	54
3.4.1	Detection of $\alpha 3$ subunit from total cell lysates.....	54
3.4.2	Detection of $\alpha 3$ and $\beta 1$ subunits from membrane preparations	56
3.5	Determination of Na,K-ATPase cell surface localization	58
3.5.1	Cytochrome c reductase assay	58
3.5.2	Na,K-ATPase activity assay	60
3.5.3	[^3H]-Ouabain binding assay	63
3.5.4	Immunofluorescence	65
4	Discussion.....	67
5	Outlook.....	72
6	References	73
7	List of figures.....	78
8	List of tables	79
9	Appendices.....	80
	Appendix A: Protein determination	80
	Appendix B: [^3H]-ouabain binding data.....	82

List of abbreviations

[³H]	tritium	MCS	multiple cloning site
7-DHC	7-Dehydrocholesterol	MD	minimal dextrose medium
aa	amino acids	MeOH	methanol
Amp	ampicillin	min	minute(s)
AOX1	alcohol oxidase 1	Miniprep	plasmid preparation
ATP	adenosine triphosphate	Mut⁺	methanol utilization plus
bidest	double distilled	Mut^S	methanol utilization slow
BMGY	buffered minimal glycerol medium	NADPH	nicotinamide adenine dinucleotide phosphate
BMMY	buffered methanol medium	n.t.c.	no template control
bp	base pairs	OD	optical density
CHO1	phosphatidylserine synthase 1	ONC	over night culture
dNTP	deoxynucleotide triphosphate	PBS	phosphate buffered saline
DHCR7	dehydrocholesterol reductase 7	PC	phosphatidylcholine
DHCR24	dehydrocholesterol reductase 24	PCR	polymerase chain reaction
DMSO	dimethyl sulfoxide	PE	phosphatidylethanolamine
DTT	dithiothreitol	PEG	polyethylene glycol
ER	endoplasmic reticulum	PI	phosphatidylinositol
ERG5	sterol C-22 desaturase	<i>P. p.</i>	<i>P. pastoris</i>
ERG6	sterol C-24 methyl transferase	PS	phosphatidylserine
EtAc	ethyl acetate	rpm	revolutions per minute
EtOH	ethanol	RT	room temperature
<i>g</i>	gravitational acceleration	s	second(s)
G418	geneticin sulfate	SDS	sodium dodecyl sulfate
GAP	glyceraldehyde-3-phosphate	SDS-PAGE	SDS-polyacrylamide gel electrophoresis
GC-MS	gas chromatography-mass spectrometry	T	temperature
GPCR	G-protein coupled receptor	TCA	trichloroacetic acid
His	histidine	TLC	thin layer chromatography
HRP	horseradish peroxidase	Trafo	transformation
IgG	Immunglobulin G	WT	wildtype
Kan	kanamycin	YNB	yeast nitrogen base
kDa	kilo Dalton	YPD	yeast extract-peptone-dextrose medium
KP_i	potassium phosphate buffer	Zeo	Zeocin TM
LB	lysogeny broth medium		

1 Introduction

Human membrane proteins are prime drug targets and, therefore, a lot of effort is put into the investigation of their structure and function [1]. Biochemical studies are often hindered by low amounts of membrane proteins that can be extracted directly from mammalian tissue. Consequently, more or less successful attempts have been made to produce sufficient amounts by heterologous expression in different host systems for characterization and crystallization studies. Expression of mammalian proteins in lower eukaryotic or prokaryotic cells often presents problems such as mistargeting and misfolding, leading to degradation of the protein [2]. Therefore, engineering of microbial hosts for better recombinant protein production is of increasing importance. The different sterol composition of mammals and yeast is considered as potential bottleneck for heterologous membrane protein expression and presents an expedient target for metabolic engineering.

1.1 Role and function of Na,K-ATPases

Since the Na,K-ATPase was discovered as a mammalian membrane protein of central function [3], its biochemical and structural properties have been studied extensively [4]. It belongs to the P-Type ATPase family of cation transporters and undertakes several essential tasks for human cell physiology. The main function is to maintain the Na^+ and K^+ gradients across the plasma membrane, which is necessary for the contractility of heart and muscle cells, as well as for neuronal excitability in the nervous tissue [5]. This is performed by transporting two K^+ ions inside the cell, while three Na^+ ions are transported outside of the cell. Lately, also additional roles as signal transducers for cell-adhesion, proliferation and apoptosis have been described for the Na,K-ATPase [6]. Moreover, the ion pump is an important target for the binding of cardiac glycosides such as ouabain and digitalis, which have been used for centuries in the treatment of heart failure. In view of these functions, it is clear that dysfunction can result in severe diseases [7].

There are four different α subunits and three different, glycosylated β subunits, which together form distinct heterodimeric human Na,K-ATPase isoforms [8]. Except isoform $\alpha 1\beta 1$, which is present ubiquitously, other isoforms are expressed in a tissue specific manner, e.g. the $\alpha 3$ subunit is mainly localized in neurons, heart and blood vessels [9,10]. Additional auxiliary subunits, belonging to the FXYD family, have been described to enhance stability in

a tissue- and isoform specific fashion. In mammals, there are seven different FXYP proteins with regulatory function [11–13].

The catalytic α subunit is responsible for ATP hydrolysis and ion transport across the membrane. It consists of ten transmembrane helices and the catalytic domain projects into the cytoplasm (see Fig. 1). By hydrolysis of one molecule of ATP, the transport of Na^+ and K^+ ions against the concentration gradient can be achieved. For this function, Mg^{2+} is needed as cofactor. The α subunit is also target for binding of cardiac glycosides such as ouabain, digoxin or digitoxin.

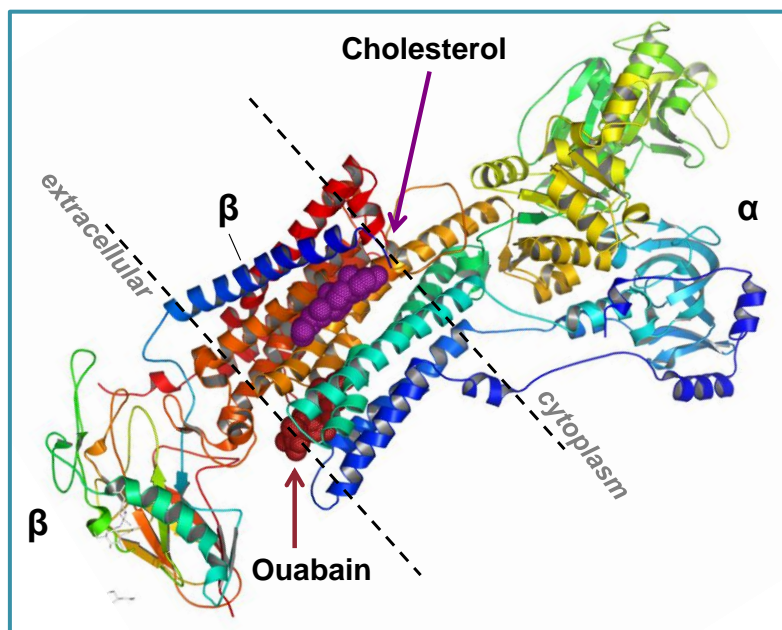


Figure 1. 2.80 Å crystal structure of Na,K-ATPase with ligands (PDB: 3A3Y).

The β subunit has only one transmembrane helix and the major part is present at the extracellular side. There are three glycosylation sites which lead to an apparent mass of 55 kDa for the peptide in mammalian cells. When expressed heterologously in yeast, the apparent maximum mass was 44 kDa only due to different glycosylation pattern. The function of the β subunit mainly comprises the stabilization of α subunit and the correct and stable assembly of the heterodimer into the plasma membrane [4,14–16].

It is difficult to isolate the different isoforms separately, so it is of main interest to express the individual functional units in organisms to facilitate purification and characterization.

Different isoforms of this enzyme have been so far expressed heterologously in *Xenopus* oocytes [17], *Saccharomyces cerevisiae* [18–20], *P. pastoris* [21,22] and insect cells [23–25].

1.2 Influence of lipids on Na,K-ATPase stability and activity

During the last years, it has become more and more obvious that cholesterol and phospholipids have a notable influence on the stability and activity of Na,K-ATPases [11,21,26–28]. Studies in which Na,K-ATPase isoforms had been expressed heterologously in different host systems revealed an essential, stabilizing role for phosphatidylserine. After purification of the protein, addition of phosphatidylserine had a strong stabilizing effect [11,28].

When cholesterol was added for activity measurements *in vitro*, the maximum specific activity could be increased [26]. Recently, cholesterol was also identified in the crystal structure of Na,K-ATPase, hence confirming the structural importance of this sterol [29]. Adamian et al. [30] showed that not only in the β 2-adrenergic receptor, but also in the Na,K-ATPase amino acid residues forming cholesterol-binding sites are strongly conserved. A cholesterol-binding consensus motif had been proposed earlier for GPCRs [31]. Findings about the interaction of sterols with membrane proteins have been extensively reviewed by Opekarová et al. [2] and Burger et al. [32]. These articles list over 30 examples for membrane proteins that require specific lipids for stability and proper function.

Considering the fact that fungi contain ergosterol while animal cells contain cholesterol as major sterol (Figure 2), it becomes clear that this situation may be a bottleneck for the heterologous expression of mammalian membrane proteins in fungi.

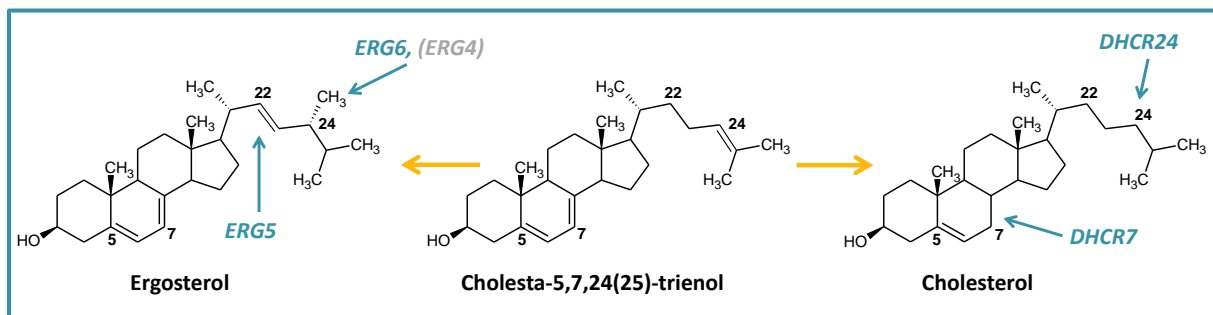


Figure 2. Structures of ergosterol and cholesterol. The enzymes involved in ergosterol synthesis are the sterol C-22 desaturase encoded by *ERG5*, the sterol C-24 methyl transferase encoded by *ERG6* and sterol C-24(28) reductase encoded by *ERG4*. For cholesterol synthesis, two dehydrocholesterol reductases are required to saturate specifically the double bonds at positions C-7 and C-24.

Despite their very similar structure, these sterols have distinct functions in biological systems as well as in artificial membranes [33]. The first steps in sterol biosynthesis are the same in animals, plants and fungi [34]. In order to synthesize ergosterol from the common intermediate zymosterol, fungi add an additional methyl group at position 24, which is accomplished by the sterol C-24 methyl transferase (Erg6p). Additionally, sterol C-24(28)-reductase (Erg4p) desaturates the double bond of this methenyl group. Furthermore, a double bond at position 22 is introduced by the sterol C-22 desaturase (Erg5p). In mammals, by contrast, sterols are saturated at positions 7 and 24 by dehydrocholesterol reductase 7 (*DHCR7*) and 24 (*DHCR24*), respectively. These small but mighty differences in the chemical structures of ergosterol and cholesterol turn out to have great influence on the biological environment of membrane proteins.

1.3 *P. pastoris* as expression host for human membrane proteins

In spite of the different membrane compounds, yeast is often preferred as expression host for mammalian membrane proteins as it is much easier and less expensive to use for recombinant protein production than mammalian or insect cells [35,36]. Still, yeasts are capable of post-translational protein modifications such as glycosylation, phosphorylation or disulfide bond formation. *P. pastoris* is especially advantageous for expression of membrane proteins as it allows high-density growth, thus enlarging the yield of recombinant protein. Furthermore, it is relatively accessible for genetic modifications and the heterologous protein expression can be strictly controlled by using the tightly regulated methanol inducible *AOX1* promoter [1,37]. Many membrane proteins, including Na,K-ATPase, have already been expressed successfully by using *P. pastoris* as host system [22,38–43].

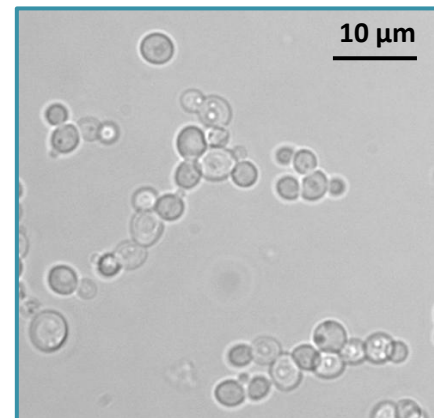


Figure 3. Microscopic image of *P. pastoris* cells.

The utility of *P. pastoris* in membrane protein expression combined with the cholesterol dependence of numerous mammalian membrane proteins triggered the interest in creating a *P. pastoris* strain capable of producing cholesterol.

Such a strain was generated by Gerald Richter [44], who followed a strategy that had lately been shown to work for *S. cerevisiae* [45]. The *P. pastoris* CBS7435 $\Delta his4\Delta ku70$ strain was engineered in its sterol pathway by knocking out two genes relevant for ergosterol synthesis (*ERG5*, *ERG6*) and by introducing two genes necessary to form cholesterol (*DHCR7*, *DHCR24*).

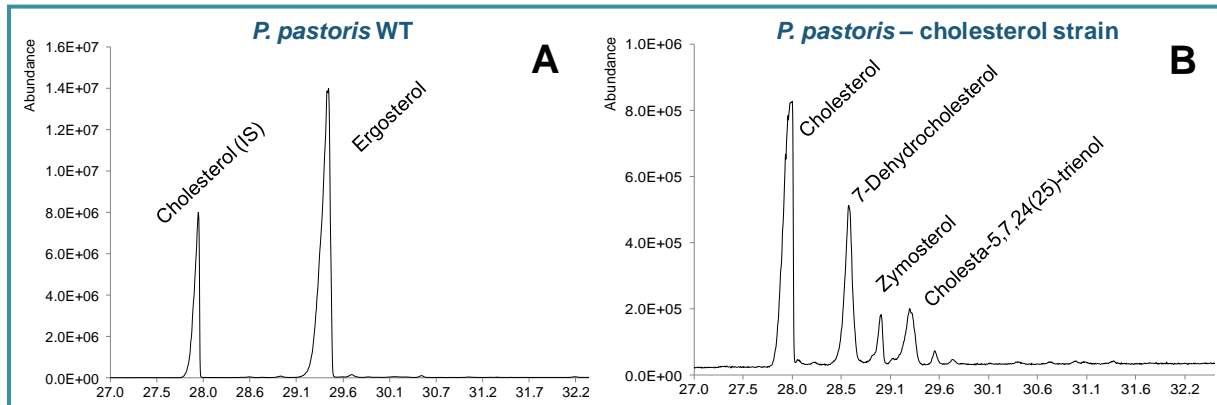


Figure 4. Sterol pattern of *P. pastoris* WT (A) and *P. pastoris* cholesterol-producing strain (B). IS = internal standard. Different compounds were identified by mass spectrometry.

The engineered *P. pastoris* strain that was used as basis for my ongoing work contained no ergosterol, but approximately 50 % cholesterol as well as intermediate products formed during sterol synthesis (see Figure 4).

1.4 Aim of this master thesis

The intention of this work was to express the mammalian membrane protein Na,K-ATPase $\alpha 3\beta 1$ isoform in different *P. pastoris* strains with altered membrane sterol composition. Main focus was thereby laid on the cholesterol-producing strain. To investigate the influence of sterols on the stability and activity of Na,K-ATPase *in vivo*, different biochemical methods were used. Expression levels of Na,K-ATPase were examined by Western blot analyses and an assay specific for Na,K-ATPase was set up to check for functionality. Finally, plasma membrane localization of Na,K-ATPase $\alpha 3\beta 1$ isoform was confirmed by radioligand cell surface binding studies using [3 H]-ouabain as well as by immunofluorescence microscopy.

A further target was to construct a *P. pastoris* $\Delta cho1$ knockout strain that should be unable to produce phosphatidylserine, which is known to have a stabilizing effect on Na,K-ATPases. As a result, stability and the specific activity of Na,K-ATPase should be influenced negatively.

2 Materials and Methods

2.1 Materials

The following section provides all reagents, media, devices, strains, vectors and primers used in this study.

2.1.1 Reagents

All reagents used in this work and the suppliers thereof are listed in Table 1.

TABLE 1. Suppliers of reagents used in this study	
Reagent	Supplier
Acetic acid (CH ₃ COOH)	Carl Roth GmbH, Germany
Acrylamid/Bis (30 %)	Sigma-Aldrich, Germany
Ammonium persulfate (APS)	Sigma-Aldrich, Germany
Bacto™ Agar	Becton, Dickinson and Company, USA
Biotin	Sigma-Aldrich, Germany
Agarose	Biozym, Germany
Ampicillin	Sigma-Aldrich, Germany
β-Mercaptoethanol	Carl Roth GmbH, Germany
Bicine	Carl Roth GmbH, Germany
Boric acid	Carl Roth GmbH, Germany
Bovine Serum Albumine (BSA)	Carl Roth GmbH, Germany
Chloroform	Carl Roth GmbH, Germany
Cholesterol	Sigma-Aldrich, Germany
CloneJET™ PCR Cloning Kit	Fermentas - Thermo Fisher Scientific, Germany
Cytochrome c	Sigma-Aldrich, Germany
dATP	Fermentas - Thermo Fisher Scientific, Germany
dCTP	Fermentas - Thermo Fisher Scientific, Germany
Deionised water	Fresenius Kabi, Austria
dGTP	Fermentas - Thermo Fisher Scientific, Germany
DMSO	Carl Roth GmbH, Germany
DreamTaq™ buffer	Fermentas - Thermo Fisher Scientific, Germany
DreamTaq™ DNA polymerase	Fermentas - Thermo Fisher Scientific, Germany
DTT	Carl Roth GmbH, Germany

dTTP	Fermentas - Thermo Fisher Scientific, Germany
EDTA	Carl Roth GmbH, Germany
Enzymes and appropriate buffers	Fermentas - Thermo Fisher Scientific, Germany
Ethanol	Australco GmbH, Austria
Ethyl acetate	Carl Roth GmbH, Germany
Ethylene glycol	Sigma-Aldrich, Germany
Folin ciocalteu phenol reagent	Merck Millipore, Germany
Formaldehyde	Carl Roth GmbH, Germany
GeneJET Plasmid Miniprep Kit	Fermentas - Thermo Fisher Scientific, Germany
GeneRuler™ 1kb Plus DNA Ladder	Fermentas - Thermo Fisher Scientific, Germany
GeneRuler™ DNA Ladder Mix	Fermentas - Thermo Fisher Scientific, Germany
Geneticin (G418) Sulfate	Invitrogen - Life Technologies
Glucose Monohydrate	Carl Roth GmbH, Germany
Glycerol	Carl Roth GmbH, Germany
Goat anti-rabbit IgG, HRP Conjugate	Invitrogen, USA
Goat anti-rabbit IgG DyLight 488 conjugate	Pierce - Thermo Fisher Scientific, Germany
[³H]-ouabain (38.4 Ci/mmol)	PerkinElmer, USA
Hydrochloric acid (HCl)	Carl Roth GmbH, Germany
Magnesiumchloride heptahydrate (MgCl₂ · 7 H₂O)	Roth GmbH, Germany
Maxima® Hot Start PCR Master Mix	Fermentas - Thermo Fisher Scientific, Germany
Methanol	Carl Roth GmbH, Germany
N,O-bis(trimethylsilyl)-trifluoroacetamide	Sigma-Aldrich, Germany
n-Heptane	Carl Roth GmbH, Germany
NADPH	Carl Roth GmbH, Germany
Ouabain octahydrate (C₂₉H₄₄O₁₂ · 8 H₂O)	Calbiochem - Merck Millipore, Germany
PageRuler™ Prestained Protein Ladder	Fermentas GmbH, Germany
Polyethylene glycol 400	Sigma Aldrich, Germany
Peptone	BD Biosciences
PMSF	Sigma-Aldrich, Germany
Phospholipid standards	Sigma-Aldrich, Germany
Phusion Buffer HF	Fermentas - Thermo Fisher Scientific, Germany
Phusion DNA Polymerase	Fermentas - Thermo Fisher Scientific, Germany
P_i Color Lock Gold Kit	Innova Biosciences, UK

Poly-L-Lysine	Sigma-Aldrich, Germany
Ponceau S (C₂₂H₁₆N₄O₁₃S₄)	Sigma-Aldrich, Germany
Potassium chloride (KCl)	Carl Roth GmbH, Germany
Potassium dihydrogen phosphate (KH₂PO₄)	Carl Roth GmbH, Germany
Potassium hydrogen phosphate (K₂HPO₄)	Carl Roth GmbH, Germany
Pyrogallol	Carl Roth GmbH, Germany
SDS	Carl Roth GmbH, Germany
Sodium hydroxide (NaOH)	Carl Roth GmbH, Germany
Sodium orthovanadate (Na₃VO₄)	Sigma-Aldrich, Germany
SuperSignal® West Pico Chemiluminescent Kit	Pierce, USA
T4 DNA Ligase and T4 DNA Ligase Buffer	Fermentas - Thermo Fisher Scientific, Germany
Trichloroacetic acid	Carl Roth GmbH, Germany
Triethylamine	Carl Roth GmbH, Germany
Tween 20	Carl Roth GmbH, Germany
Ultima-Gold Scintillation Cocktail	PerkinElmer, USA
Vectashield Mounting Medium	Vector Laboratories
Wizard® SV Gel and PCR Clean-Up System	Promega
Yeast Extract	Carl Roth GmbH, Germany Bacto Laboratories Pty Ltd, Australia
Zymolyase	AMS Biotechnology, UK

2.1.2 Media and buffers

The different solutions, buffers and media used in this work are listed in Table 2.

TABLE 2. Solutions and Media used		
<i>E. coli</i> media	LB ^{Amp} agar plates	10 g/l tryptone, 5 g/l yeast extract, 10 g/l NaCl, 15 g/l agar, 100 mg/l ampicillin
	SOC medium	20 g/l bacto tryptone, 0.58 g/l NaCl, 5 g/l bacto yeast extract, 2 g/l MgCl ₂ , 0.16 g/l KCl, 2.46 g/l MgSO ₄ , 3.46 g/l dextrose
<i>P. pastoris</i> Trafo	BEDS (10 ml)	1 ml of 0.1 M bicine NaOH (10 x), 300 µl of ethylene glycol, 500 µl of DMSO, 2 ml of 5 M sorbitol, 6.2 ml of H ₂ O
	0.1 M Bicine NaOH, pH 8.3	1.63 g N,N-Bi-(2-hydroxyethyl)-glycine in 100 ml H ₂ O
	1 M DTT	1.54 g dithiothreitol dissolved in 10 ml H ₂ O
	5 M sorbitol	91.1 g sorbitol in 100 ml H ₂ O

Yeast cultivation and selection media	500 x biotin	0.2 g/l biotin
	10 x YNB	134 g/l yeast nitrogen base with ammonium sulfate without amino acids
	10 x glycerol	100 ml of glycerol, 900 ml of H ₂ O
	10 x D-glucose	200 g/l D-glucose
	1 M potassium phosphate buffer, pH 6.0	132 ml of 1 M K ₂ HPO ₄ (174.18 g/l), 868 ml of 1 M KH ₂ PO ₄ (136.09 g/l)
	MD-His agar plates	15 g/l agar, 100 ml of 10 x YNB, 2 ml of 500 x Biotin, 100 ml of 10 x D-glucose, 800 ml of H ₂ O
	MD-His Zeo agar plates	15 g/l agar, 100 ml of 10 x YNB, 2 ml of 500 x Biotin, 100 ml of 10 x D-glucose, 800 ml of H ₂ O, 100 mg/l Zeocin
	BMGY medium	10 g/l yeast extract, 20 g/l peptone, 100 ml of 1 M potassium phosphate buffer pH 6.0, 100 ml of 10 x YNB, 2 ml of 500 x Biotin, 100 ml of 10 x Glycerol, 700 ml of H ₂ O
	BMMY medium	10 g/l yeast extract, 20 g/l peptone, 100 ml of 1 M potassium phosphate buffer pH 6.0, 100 ml of 10 x YNB, 2 ml of 500 x Biotin, 700 ml of H ₂ O, methanol for desired concentration
	Breaking Buffer, pH 7.4	6 g/l sodium phosphate (monobasic), 372 mg/l EDTA, 50 ml of glycerol, 900 ml of H ₂ O, 1 mM PMSF (added freshly)
	YPD	10 g/l yeast extract, 20 g/l peptone, 20 g/l agar, 100 ml of 10 x D-glucose
	YPD-Hyg	YPD medium + 100 mg/l hygromycin
SDS-PAGE and Western blot	10 x SDS running buffer	28 g/l Tris, 144 g/l Glycin, 10 g/l SDS
	20 x transfer buffer	29 g/l Tris, 144 g/l Glycin
	1 x transfer buffer	50 ml of 20 x transfer buffer, 100 ml of methanol, 850 ml of H ₂ O
	10 x TBS buffer, pH 7.5	30.3 g/l Tris, 87.6 g/l NaCl, pH adjusted with HCl
	1 x TBST buffer	100 ml of TBS buffer, pH 7.5, 300 µl of Tween [®] 20, filled to 1 l with water
	TBST - milk	5 g whey powder per 100 ml 1x TBST
	Tris-HCl buffer, pH 6.8	60.5 g/l Tris, pH adjusted with HCl
	Tris-HCl buffer, pH 8.8	181.7 g/l Tris, pH adjusted with HCl
	SDS-PAGE sample buffer	780 µl dissociation buffer, 200 µl Tris-HCl buffer, pH 8.8, 20 µl β-mercaptoethanol
	Dissociation buffer	20 mM KH ₂ PO ₄ , 6 mM EDTA, 6% SDS, 10% glycin, 0.05% bromophenol blue

Biochemical Assays	TE-buffer, pH 7.5	10 mM Tris, 1 mM EDTA, pH adjusted with HCl
	Tris-HCl buffer, pH 7.4	10 mM Tris, pH adjusted with HCl
	Cyt-c reductase assay buffer	300 mM potassium phosphate buffer, pH 7.8, containing 0.1 mM EDTA
	Enzyme dilution buffer	Cyt-c reductase Assay buffer with 0.5 mg/ml BSA
	Cyt-c oxidase inhibitor solution	50 mM potassium cyanide (KCN) in water
	NADPH Stock Solution	40 mg/ml NADPH in water
	ATPase Assay reaction mix	130 mM NaCl, 20 mM KCl, 3 mM MgCl ₂ , 1 mM EDTA, 25 mM histidine, pH 7.4, (with or without 10 mM ouabain), ATP was added freshly to 0.1 mM
	[³ H]-ouabain binding buffer	1 M sorbitol, 3 mM Mg ₂ SO ₄ , mM EDTA, 10 mM Tris-HCl, pH 7.4, 1 mM NaTris ₂ VO ₄ and [³ H]-ouabain (various conc.) was added freshly
Lowry-method	Solution A	200 µl of 2.2 % Disodium tartrate, 200 µl of 1 % CuSO ₄ · 5 H ₂ O, 500 µl of 20 % SDS and 20 ml of 2 % Na ₂ CO ₃ in 0.1 M NaOH
	Solution B	Folin Ciocalteu phenol reagent/H ₂ O (1:1)
	Solution C	0.1 % SDS in 0.1 M NaOH
Immunofluorescence	100 mM potassium phosphate buffer, pH 7.5	32 ml of 0.2 M KH ₂ PO ₄ , 168 ml of 0.2 M K ₂ HPO ₄ , 200 ml H ₂ O
	Solution B	1.2 M sorbit in 100 mM KP _i , pH 7.5
	Solution C	1.2 M sorbit (218.6 g/l) in H ₂ O
	PBS Albumin	100 mM KP _i , 2 % BSA, pH 7.5
	Blocking Solution	40 mM K ₂ HPO ₄ , 10 mM KH ₂ PO ₄ , 150 mM NaCl, 0.1% NaN ₃ , 0.1% Tween [®] 20, 2 % whey powder
	Formalin	37% Formaldehyde in H ₂ O

2.1.3 Instruments and devices

Table 3 lists all instruments and devices used for the experiments.

TABLE 3. Instruments and Devices used in this work.		
Task	Instrument/Device	Manufacturer
Absorption measurement	Microplate Reader Spectramax Plus 384	Molecular Devices, Germany
	96-well Micro plates MICROLON [®] DU-800 Spectrophotometer	Greiner bio-one GmbH, Germany Beckman Coulter, Ireland
Cell harvest and membrane preparation	MSK Homogenizer	Braun, Germany
	Hand homogenizer	Sartorius AG, Germany
	Eppendorf table top centrifuge 5810R	Eppendorf, Germany
	Eppendorf Micro centrifuge 5415R	Eppendorf, Germany
	Avanti [™] J-20 XP Centrifuge, JA-25.50 rotor and Optima [™] LE-80K Ultracentrifuge, Ti70 rotor	Beckman Coulter [™] , USA
DNA-concentration	NanoDrop 2000c Spectrometer,	PEQLAB Biotechnologie, Germany
Electrophoresis	PowerPac [™] Basic + Sub-Cell GT	BIO-RAD, USA
Electroporation	MicroPulser [™]	BIO-RAD, USA
	Electroporation Cuvettes (2 mm gap)	Molecular BioProducts Inc., USA
Cell cultivation	50 ml Greiner tube	Greiner bio-one, Germany
	300 ml shaking flasks with baffles	
	2 l shaking flasks with baffles	
GC-MS	Hewlett Packard 5890 Series II with a MS detector; HP 5 MS Column (Capillary 28.8 m x 0.25 mm x 0.25 µm film)	Agilent Technologies, Austria
Incubator	BINDER Kühlbrutschränke	Binder GmbH, Germany
Lipid Extraction	Pyrex [®] tubes (10 ml)	Sigma-Aldrich, USA
	Vibrax VXR basic	IKA [®] , Germany
Liquid Scintillation counting	Tri-Carb 2900TR	Packard/PerkinElmer, USA
Microscopy	Leica DM LB2/DFC350 FX camera	Leica Microsystems, Germany
	Neubauer Improved Hemocytometer	Superior Marienfeld, Germany
OD₆₀₀ measurement	BioPhotometer Plus	Eppendorf, Germany
	Cuvettes (10 x 4 x 45 mm)	Sarstedt, Germany
PCR reaction	GeneAmp [®] PCR System 2700	Applied Biosystems, USA
Plate shaker	GFL 3013	GFL GmbH, Germany
SDS-PAGE	Xcell SureLock [™] Mini-Cell	Invitrogen, USA
	PowerEaseR 500 Power Supply	Invitrogen, USA

Shaker for cell cultures	HT Multitron II	Infors AG, Switzerland
Sterile bench	Uniflow KR130	UniEquip, Germany
Thermo-mixing	Thermomixer comfort	Eppendorf, Germany
Western blot	XCell SureLock™ Mini-Cell	Invitrogen, USA
	Nitrocellulose membrane, Hybond-ECL™	Amersham Biosciences, Sweden
	G:Box BioImaging HR	Syngene, UK
Weighing	Lab scale: TE 1502S	Sartorius, Germany
	Precision scale: Explorer	Ohaus, Germany

2.1.4 Strains

The different *P. pastoris* and *E. coli* strains used in this work are described in Table 4.

TABLE 4. <i>P. pastoris</i> and <i>E. coli</i> strains used in this study			
Name	Background	Phenotype	Source
<i>P. p.</i> WT	<i>P. pastoris</i> CBS7435 $\Delta his4\Delta ku70$	Histidin auxotrophy	Laura Näätsaari [46]
<i>P. p.</i> SMD1186	<i>P. pastoris</i> SMD1168 $\Delta his4\Delta pep4$	Protease deficient strain	Invitrogen
<i>P. p.</i> $\Delta erg5::DHCR7$	$\Delta erg5::pPpGAP-Zeo[DHCR7]^a$	Campesterol producing strain	Gerald Richter
<i>P. p.</i> $\Delta erg6::DHCR24$	$\Delta erg6::pPpGAP-Kan[DHCR24]^a$	7-DHC producing strain	Gerald Richter
<i>P. p.</i> $\Delta erg5::DHCR7$ $\Delta erg6::DHCR24$	$\Delta erg5::pPpGAP-Zeo[DHCR7]$ $\Delta erg6::pPpGAP-Kan[DHCR24]^a$	Cholesterol-producing strain	Gerald Richter
<i>P. p.</i> $\Delta erg6$	$\Delta erg6::pFA6KanMX6[erg6]$	Cholesta-5,7,24-trienol producing strain	Tamara Wriessnegger
<i>P. p.</i> <i>DHCR7</i>	$PpGAPZA[DHCR7]^a$	Brassicasterol producing strain	Tamara Wriessnegger
<i>P. p.</i> S- $\alpha 3\beta 1$	<i>P. pastoris</i> SMD1168	Contains $\alpha 3\beta 1$ expression cassette	Cristina Reina [22]
Name	Genotype	Source	
<i>E. coli</i> Top10F'	$F'\{lacI^q Tn10 (Tet^R)\} mcrA \Delta(mrr-hsdRMS-mcrBC) \Phi 80 lacZ\Delta M 15 \Delta lacX74 recA1 araD139 \Delta(ara-leu)7697 galU galK rpsL endA1 nupG$	Invitrogen	

^a Strains were derived from *P. pastoris* CBS7435 $\Delta his4\Delta ku70$.

2.1.5 Vectors

The vector pAO815- $\alpha 3\beta 1$ used for transformation into electrocompetent *P. pastoris* cells was kindly provided by Cristina Reina (Prassis Sigma Tau Research Institute, Milan). The plasmid contains the genes for the $\alpha 3$ and $\beta 1$ subunits of Na,K-ATPase. Expression is inducible with methanol because of the *AOX1* promoter. The *HIS4* gene is used as auxotrophic marker. The vector was linearized prior to transformation with *Bgl*II (Figure 5).

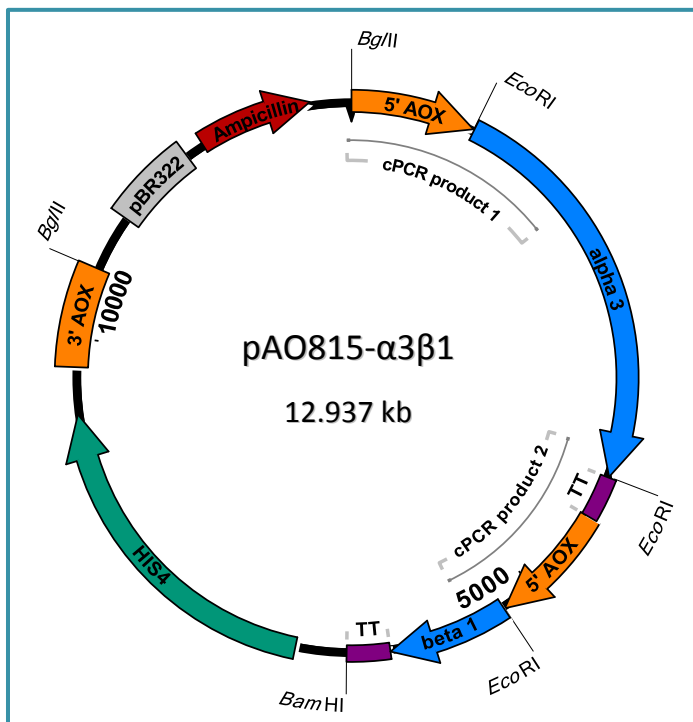


Figure 5. Expression vector pAO815- $\alpha 3\beta 1$. The vector contains both subunits of Na,K-ATPase under the control of *AOX1* promoters and the *HIS4* auxotrophic marker for expression in *P. pastoris* as well as an ampicillin resistance and origin of replication for amplification in *E. coli*. Restriction sites and primer binding sites for colony PCRs are indicated in the vector map.

The vector pAG32-HPH (Figure 6) was used for the construction of the *CHO1* knockout cassette. It provides a hygromycin resistance gene under the control of a TEF promoter and a TEF terminator. The disruption cassette was amplified via PCR using the primers listed in Table 6.

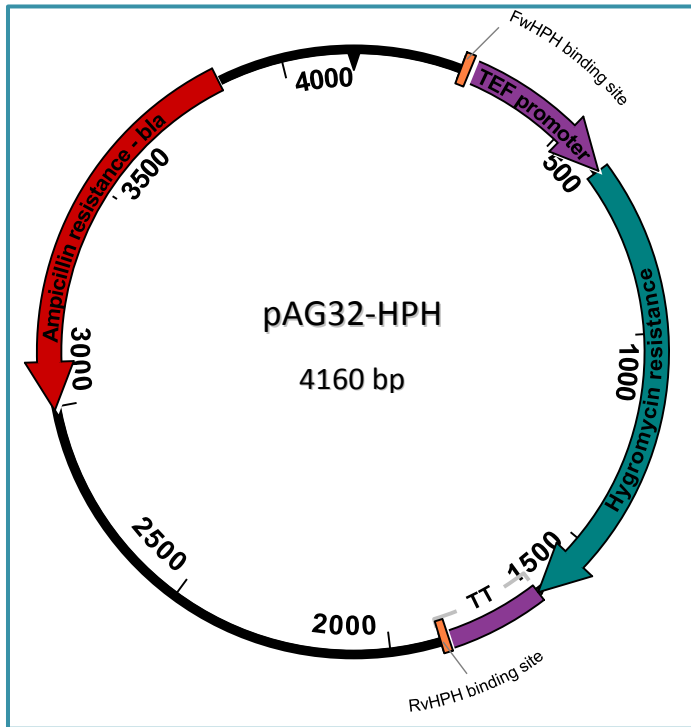


Figure 6. Expression vector pAG32-HPH. The vector contains the hygromycin resistance gene (*HPH*) under the control of *TEF* promoter and *TEF* terminator for selection in *P. pastoris*. The *HPH* sequence was amplified with primers FwHPH and RvHPH for construction of the *CHO1* knockout cassette.

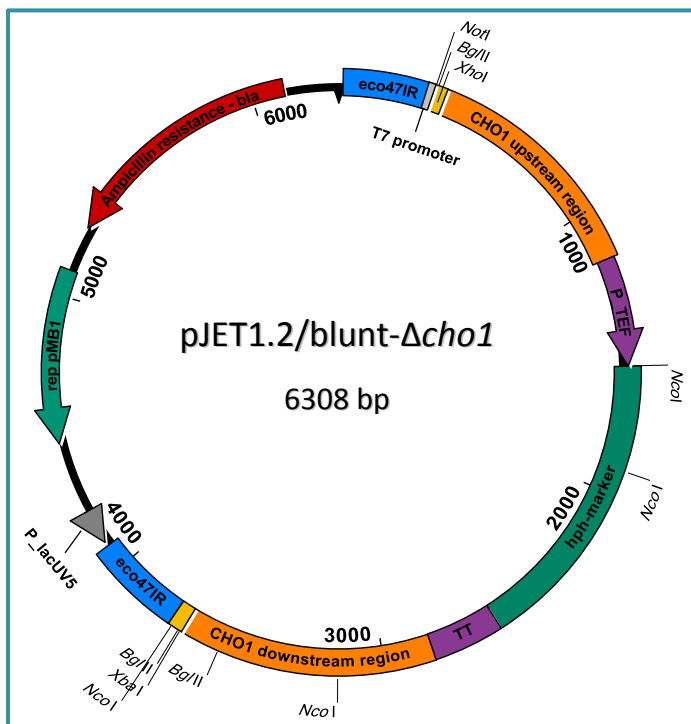


Figure 7. pJET1.2/blunt- Δ cho1 vector. The vector contains the *CHO1* knockout cassette with 5' and 3' up- and downstream regions. *HPH* was used as selection marker as it is responsible for hygromycin resistance in *P. pastoris*. An ampicillin resistance gene and the origin of replication pMB1 are necessary for amplification in *E. coli*.

For generating the *P. pastoris* Δ *cho1* knockout strain, the cassette was cloned into pJET1.2/blunt (Figure 7) to be able to amplify sufficient amounts for transformation via PCR. The construct was furthermore used for sequencing of the knockout cassette.

2.1.6 Primers

Primers used in this study are listed in Tables 5-8. The primers were diluted to a final concentration of 10 μ M.

Example for dilution:

The delivered primer contained 28.6 nmol. Therefore, 286 μ l of H₂O were added to obtain a concentration of 100 μ M. The oligonucleotides were dissolved at 65 °C and 600 rpm for 10 min. Then, 20 μ l of the diluted primer were mixed with 180 μ l of H₂O to get a concentration of 10 μ M.

TABLE 5. Primers for cPCR verification of *P. pastoris* transformants containing pAO815- α 3 β 1

Name of primer	Sequence 5'-3'	T _m	Product size
<i>Fwd_AOXdown</i>	GACGCAGATCGGGAACACTG	68.5 °C	1899 bp
<i>Rev_Alpha3</i>	CGAGAATGAGGGAGAGGATGAAG	67.5 °C	
<i>Fwd_alpha3</i>	TCGGGCTGTTTGAGGAGAC	65.9 °C	1772 bp
<i>Rev_beta1</i>	GCTCTGGGATCATTAGGACGAAAG	68,7 °C	

TABLE 6. Primers for construction of *CHO1* knockout cassette

Name of primer	Sequence 5'-3'	T _m	Product size
<i>Fw_cho1_up</i>	TGTTGGTGGATCAACTACAAAATC	63.9 °C	829 bp
<i>Rev_cho1_hph</i>	<u>CCCGCGGGGACAAGGCAAGCT</u> CCTTAGAAGCCAT TAGGAGCTTTG ^a	87.6 °C/ 62.4 °C ^b	
<i>Fw_cho1_hph</i>	CGATACTAACGCCGCCATCCAGTGTCTGAATATGGA <u>TATGGTTGCATTATCAGAG</u> ^c	88.9 °C/ 63.0 °C ^b	906 bp
<i>Rev_cho1_down</i>	AAGAGGATGTCGAGAACTTCGAG	65.2 °C	
<i>FwHPH</i>	AGCTTGCCTTGTCGCCGCCG	76.5 °C	1648 bp
<i>RvHPH</i>	TCGACACTGGATGGCGGCG	75.6 °C	

^a The underlined sequence binds to TEF promoter region of pAG32-hph vector for overlap extension PCR.

^b Melting temperature of whole primer and of sequence binding to *CHO1* region, respectively.

^c The underlined sequence binds to TEF terminator region of pAG32-hph vector for overlap extension PCR.

TABLE 7. Primers for cPCR verification of *P. pastoris* Δ cho1 knockout mutants

Name of primer	Sequence 5'-3'	T _m	Product size
<i>Fw_cho1_genom</i>	GCTGGCTCACATCTCGTATTC	51.4 °C	1387 bp
<i>Rv_TEFpromoter</i>	GTTGTTTATGTTCCGGATGTGATG	51.3 °C	
<i>Fw_hph_marker</i>	AGAAGTACTCGCCGATAGTGG	62.6 °C	1284 bp
<i>Rv_cho1_genom</i>	TCGGATTTTGGCAGTTACAG	63.0 °C	
<i>Fw_cho1cds</i>	CTCAGTTCGAGGGGAATCAG	64.2 °C	781 bp
<i>Rv_cho1cds</i>	TTTGGAGGTCATCAAACATCC	64.0 °C	

TABLE 8. Primers for Sequencing of *P. pastoris* Δ cho1 knockout mutants

Name of primer	Sequence 5'-3'	T _m
<i>pJET1.2/blunt Fwd</i>	CGACTCACTATAGGGAGAGCGGC	64.2 °C
<i>Rev_TEF_promoter</i>	GTTGTTTATGTTCCGGATGTGATG	51.3 °C
<i>Fwd_SequencingCho1</i>	TGCCACTGAGGTTCTTCTTTC	63.7 °C
<i>Fwd_hph_marker</i>	AGAAGTACTCGCCGATAGTGG	62.6 °C
<i>Rv_SequencingCho1</i>	CTATACAAATGACAAGTTCTTG	53.0 °C
<i>pJET1.2/blunt Rev</i>	AAGAACATCGATTTTCCATGGCAG	64.4 °C

2.2 Methods

The following section describes general methods as well as particular techniques that were carried out during this work.

2.2.1 General methods

2.2.1.1 Electrocompetent *E. coli* cells

Overnight cultures of *E. coli* TOP10F' cells were inoculated in 30 ml of LB media at 37 °C and 220 rpm. For the main culture, 500 ml of LB media were inoculated with 5 ml of the ONC in 2 l baffled flasks. Cells were incubated at 37 °C and 170 rpm until an OD₆₀₀ value between 0.7 and 0.9 was reached. Cultures were pre-chilled on ice for 30 min before harvesting by centrifugation for 15 min at 2000 x *g* and 4 °C. Pellets were washed twice with 500 ml of ice-cold H₂O and centrifuged as described above. The cells were resuspended in 35 ml of pre-chilled, sterile 10 % glycerol and centrifuged for 15 min at 4000 x *g* and 4 °C. Finally, pellets were resuspended in 1 ml of ice-cold 10 % glycerol. Aliquots containing 80 µl of electrocompetent cells were quick-frozen with liquid nitrogen and stored at -80 °C until use.

2.2.1.2 Transformation of *E. coli* cells

For electroporation of *E. coli* TOP10F' cells, 50 µl of electrocompetent cells were mixed with 2 µl of plasmid DNA and transferred to pre-chilled electroporation cuvettes. Cells were pulsed for 5-6 ms with the electroporator set to program EC2 at 2.5 kV. One ml of SOC medium was immediately added after transformation and cells were incubated at 600 rpm and 37 °C for 30 min. Cells were shortly spun down in the microcentrifuge and resuspended in the remaining media. The whole suspension was plated on LB^{Amp} agar plates and incubated at 37 °C overnight. *E. coli* strains harboring the Na,K-ATPase expression vector and the pJET1.2/blunt_Δ*cho1* plasmid were used for amplification and sequencing of the constructs.

2.2.1.3 Plasmid isolation

Isolation of the pAO815-α3β1 or pJET1.2/blunt_Δ*cho1* vector from *E. coli* TOP10F' cells was performed as described in the manual of GeneJET™ Plasmid Miniprep Kit. For each miniprep, fresh *E. coli* cells were grown on LB^{Amp} plates over night at 37 °C. The DNA was eluted with 50 µl nuclease-free water. To estimate the amount of isolated plasmid DNA, 1 µl

of the sample was mixed with 1 μ l of 6 x loading dye and 4 μ l of water. The samples were analyzed on a 1 % agarose gel.

2.2.1.4 Agarose gel electrophoresis

For agarose gel electrophoresis, a 1 % gel was poured using 2 g of agarose and 200 ml of 1 x TAE buffer. Ethidium bromide was added to make DNA bands visible. For control gels, 5 μ l of a DNA standard (Figure 8) were loaded and the gel was run for 45 min at 120 V. For preparative agarose gels, 10 μ l of DNA standard were loaded and the gel was run for 1.5 h at 90 V.

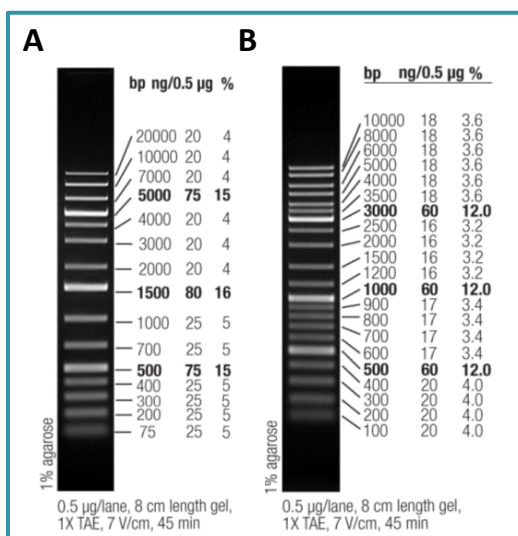


Figure 8. GeneRuler™ 1 kb Plus DNA Ladder (A) and GeneRuler™ DNA Ladder Mix (B) were used as size standards for agarose gel electrophoresis.

2.2.1.5 Vector linearization

Prior to transformation into *P. pastoris* cells, the vector pAO815 α 3 β 1 had to be linearized with *Bgl*II:

10 μ l plasmid pAO815 α 3 β 1 (concentration about 150 ng/ μ l)

2 μ l *Bgl*II

2 μ l buffer orange (10 x)

6 μ l H₂O

20 μ l total volume

Linearization was performed at 37 °C over night. After linearization, the whole reaction mixture was loaded onto a preparative agarose gel and purified afterwards with “Wizard® SV Gel and PCR Clean-Up” System. One μ l of the samples was then loaded onto an agarose gel to be able to estimate the concentration. In some cases, the amount was hard to estimate on the gel. Consequently, the concentration was additionally determined with the NanoDrop™ micro-volume spectrophotometer device.

2.2.1.6 Transformation of electrocompetent *P. pastoris* cells

For transformation of different *P. pastoris* strains, ONCs were usually grown in 10 ml BMGY medium at 28 °C and 100-120 rpm over night. Main cultures were inoculated to an OD₆₀₀ of 0.05-0.2 in 50 ml BMGY in baffled shaking flasks, depending on whether the cultures were grown over night or during the day. Because of the different growth rates of the strains, it was difficult to estimate when the optimal OD₆₀₀ of 0.8-1 would be reached. For preparation of competent cells, the cultures were centrifuged for 5 min at 500 x *g* and resuspended in 9 ml BEDS and 1 ml DTT. The cells were incubated for 5 min at 28 °C and 100 rpm. Then, they were centrifuged for 5 min at 500 x *g* and resuspended in 1 ml BEDS.

An aliquot of 80 µl of competent cells was mixed with 500-1000 ng linearized DNA (about 10-20 µl of linearized pAO815α3β1 or *CHO1* knockout cassette, respectively) and incubated on ice for 5 min. Water was used instead of DNA for the negative control. The cells were pulsed using an electroporator with the settings: 1500 V, 200 Ω and 25 µF. Immediately after the pulse, 500 µl of ice cold 1 M sorbitol and 500 µl of BMGY medium were added to the cells. Transformants were recovered for 1-3 h at 28 °C and plated on MD-His plates (in case of pAO815-α3β1 vector) or YPD-Hyg plates (in case of *CHO1* knockout cassette). Usually, 50 µl, 100 µl and the rest, after a short centrifugation step, were plated and incubated at 28 °C for several days until colonies appeared.

2.2.1.7 Growth curves

For growth analytics, precultures of *P. pastoris* strains were grown in 10 ml BMGY at 28 °C and 120 rpm over night. The main cultures were inoculated to an initial OD₆₀₀ of 0.1 in 300 ml baffled shaking flasks filled with 50 ml of BMGY media. Samples were taken every 3 h during logarithmic growth phase and every 2 h during stationary phase over a total time period of 56 h. OD₆₀₀ values were measured by a spectrophotometer and data was plotted on a logarithmic scale. Samples were diluted with BMGY if it was necessary. The specific growth rate μ was calculated when cells were in the exponential growth phase as shown in Equation 1.

$$\mu = \frac{\Delta \ln(\text{OD}_{600})}{\Delta t} \quad (\text{Equation 1})$$

2.2.1.8 Preparation of glycerol stocks

To preserve the positive transformants of *P. pastoris* Na,K-ATPase producing strains or $\Delta cho1$ knockout strains, glycerol stocks were made. Single colonies were grown in 10 ml BMGY over one or two nights and centrifuged at $2500 \times g$ for 5 min. The cells were resuspended in 1 ml BMGY and transferred to CryoTubes. Five hundred μ l of 50 % glycerol were added to the cells and incubated for 30 min at room temperature. The cells were frozen rapidly with liquid nitrogen and stored at -80°C .

2.2.2 Construction of *P. pastoris* knockout and expression strains

2.2.2.1 Construction of *CHO1* knockout cassette via overlap extension PCR

In order to generate a *P. pastoris* strain which lacks the phosphatidylserine synthase, a knockout cassette was constructed (Figure 9).

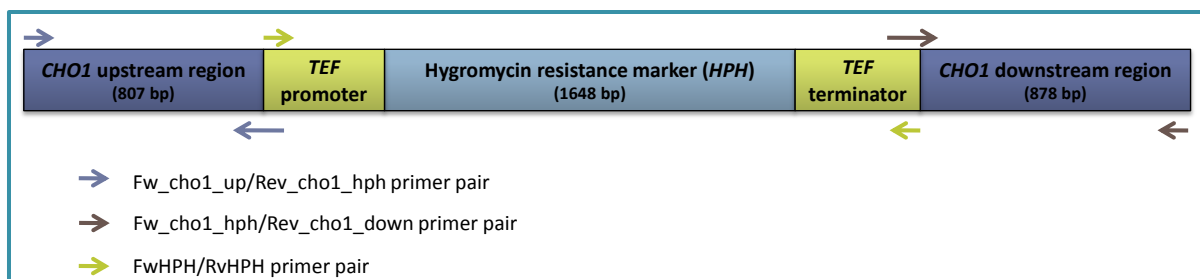


Figure 9. Phosphatidyl serine synthase (*CHO1*) knockout cassette used for transformation into electrocompetent *P. pastoris* cells. Binding sites of primers used for overlap extension PCR are indicated.

First of all, the fragment with the *TEF* promoter, the *HPH* gene and *TEF* terminator was amplified from the vector pAG32-HPH via PCR. Therefore, the primers FwHPH and RvHPH were used. The PCR reaction was set up as follows:

- 30 μ l H₂O
- 1 μ l template DNA (pAG32-hph plasmid)
- 2 μ l forward primer (FwHPH)
- 2 μ l reverse primer (RvHPH)
- 5 μ l dNTPs
- 10 μ l Polymerase buffer (F-518 5 x Phusion HF + 7.5 mM MgCl₂)
- 0.4 μ l Phusion Polymerase (Finnzyme)

- 50.4 μ l total volume

To amplify the upstream and downstream regions of the *CHO1* gene, the primer pairs Fw_cho1_up/Rev_cho1_hph and Fw_cho1_hph/Rev_cho1_down were used. The PCR reaction was set up as follows:

30 µl H₂O
1 µl template DNA (*P. pastoris* genomic DNA)
2 µl forward primer (Fw_cho1_up or Fw_cho1_hph)
2 µl reverse primer (Rev_cho1_hph or Rev_cho1_down)
5 µl dNTPs
10 µl Polymerase buffer (F-518 5 x Phusion HF + 7.5 mM MgCl₂)
0.4 µl Phusion Polymerase (Finnzymes)
50.4 µl total volume

Water was used instead of DNA for a no template control.

PCR cycling conditions:

98 °C 30 s
98 °C 10 s }
62 °C 30 s } 30 cycles
74 °C 1 min }
74 °C 7 min }
4 °C ∞

After the PCR reaction, the whole mixture was loaded onto a preparative agarose gel and purified with “Wizard® SV Gel and PCR Clean-Up” System. To estimate the amount of DNA, a control gel was run after purification. To create the final construct, an overlap extension PCR was performed. The PCR mixture consisted of the following:

0.4 µl Phusion Polymerase (Finnzymes)
5 µl dNTPs
2.6 µl H₂O
2 µl forward primer (Fwd_cho1_up)
2 µl reverse primer (Rev_cho1_down)
10 µl Polymerase buffer (F-518 5 x Phusion HF + 7.5 mM MgCl₂)
7 µl *CHO1* upstream fragment
7 µl *CHO1* downstream fragment
14 µl hph fragment from pAG32-hph vector
50 µl total volume

PCR cycling conditions:

98 °C 30 s
98 °C 10 s
55 °C/64 °C 30 s } 30 cycles
74 °C 2 min
74 °C 7 min
4 °C ∞

After PCR, the total volume was purified over agarose gel electrophoresis and “Wizard® SV Gel and PCR Clean-Up” System. One µl of the cleaned DNA fragment was loaded onto a control gel to estimate the concentration.

2.2.2.2 Sequencing of *CHO1* knockout cassette

Prior to transformation into *P. pastoris*, the *CHO1* knockout cassette had to be sequenced to confirm the lack of mutations. For this purpose, and to be able to amplify the cassette to obtain sufficient amounts for transformation into *P. pastoris*, the construct was cloned into pJET1.2/blunt vector (see Figure 7) via blunt end ligation. To achieve blunt end ligation the CloneJET™ PCR cloning kit was used with the following setup:

10 µl 10 x reaction buffer
2 µl PCR product (*CHO1* knockout cassette)
1 µl linear pJET1.2/blunt vector
1 µl T4 DNA Ligase
6 µl H₂O
20 µl total volume

The reaction mix was incubated for 10 min at RT and 2 µl were transformed into *E. coli* TOP10F' cells according to chapter 0. Isolated plasmids were used for sequencing of the knockout cassette. Four µl of respective sequencing primers (see Table 8) at a concentration of 5 pmol/µl were added to 10 µl of pJET1.2/blunt-*Δcho1* (100 ng/µl) and samples were sent to LGC genomics (Germany) for sequencing.

2.2.2.3 Colony PCR

The knockout cassette was transformed into electrocompetent *P. pastoris* cells according to section 2.2.1.6. Positive transformants of *P. pastoris* were streaked out freshly onto selective media plates and grown at 28 °C for a few days. A little bit of cell material from a single colony was then resuspended in 25 µl of sterile H₂O, incubated at 95 °C for 5 min and chilled

on ice for another 5 min. The cell suspension was centrifuged for 30 s at max. speed and 1.5 μ l of the supernatant were used for colony PCR. The primers used for colony PCR are listed in Table 7.

Reaction set-up:

1.5 μ l supernatant from colony
1 μ l forward primer
1 μ l reverse primer
12.5 μ l Hot Start Maxima Master Mix (Fermentas)
9 μ l H₂O

25 μ l total volume

PCR cycling conditions:

95 °C 4 min
95 °C 30 s
55 °C 30 s } 30 cycles
72 °C 2 min }
72 °C 7 min
4 °C ∞

2.2.3 Lipid analysis

2.2.3.1 Extraction and GC-MS analysis of total sterols from yeast

The *P. pastoris* strains used in this work were analyzed with GC-MS to determine the sterol compounds in the membrane. ONCs of the strains were grown in 10 ml YPD and 15 OD₆₀₀ units were harvested by centrifugation for 5 min at 1250 x *g*. Then, 600 μ l of methanol, 400 μ l of pyrogallol (0.5 % dissolved in methanol, prepared freshly) and 400 μ l of 60 % aqueous KOH were added to the samples. Five μ l of cholesterol standard (2 mg/ml) were added to all samples except for the strain that was expected to produce cholesterol. The pellet was dispersed by vortexing and heated for 2 h in a sand bath at 90 °C. Lipids were extracted by adding 1 ml n-heptane and centrifugation for 3 min at 450 x *g*. The upper phase containing the lipid extract was transferred to a fresh Pyrex tube. This step was repeated 3 times. The extracts were dried under a N₂ stream and then dissolved in 10 μ l of pyridine. For derivatization, 10 μ l of N'-bis(trimethylsilyl)-trifluoroacetamide were added and incubated for 10 min. Then, 50 μ l of ethyl acetate were added and the samples were analyzed via GC-

MS (performed by Erich Leitner, Institute of Analytical Chemistry and Food Chemistry, TU Graz). For technical data on GC-MS analysis, see Table 9.

TABLE 9. Adjustments for GC-MS analysis of total sterols from *P. pastoris*

GLC	HP 5890 Series II Plus with Electronic Pressure Control and 6890 automated liquid sampler (ALS)
Injector	Split/splitless 270 °C, mode: splitless, purge on: 2 min
Injection volume	1 µl
Column	HP 5-MS (Crosslinked 5% Phenyl Methyl Siloxane), 30 m x 0.25 mm i.d. x 0.25 µm film thickness
Carrier	Helium, 5.0
Flow	0.9 ml, linear velocity 35.4 cm/s, constant flow
Oven	100 °C (1 min), ramp of 10 °C/min to 250 °C (0 min) and ramp of 3 °C/min to 300 °C (0 min)
Detector	Selective detector HP 5972 MSD
Ionization	EI, 70 eV
Mode	Scan, scan range: 100-550 amu, 2.58 scans/s
EM Voltage	Tune voltage
Tune	Auto tune

2.2.3.2 Extraction and thin layer chromatography of yeast phospholipids

Phospholipids were extracted from cell homogenates after glass-bead disruption (see section 2.2.4.2) according to the protocol described by Schneiter and Daum [47]. Briefly, 4 ml of CHCl₃/MeOH (2:1) were added and lipids were extracted by vigorous shaking on the Vibrax for 1 h. Two ml of a 0.034 % aqueous MgCl₂ solution were added and samples were washed for 2 min on the Vibrax. After centrifugation for 3 min at 1250 x *g*, the upper phase, containing non-lipid contaminants, was removed. Extracts were washed with 2 ml of 2 N KCl/MeOH (4:1) for 2 min on the Vibrax. Samples were again centrifuged for 3 min at 1250 x *g*. A third washing step with 1.5 ml of artificial upper phase, consisting of CHCl₃/MeOH/H₂O (3:48:47) was conducted for 2 min on the Vibrax. The aqueous and organic phases were again separated by centrifugation for 3 min at 1250 x *g* and the upper phase as well as the interphase, mainly composed of precipitated proteins, was removed. The organic

phase was dried under a stream of nitrogen and lipid extracts were dissolved in 20 μl of CHCl_3 :MeOH (2:1).

Separation of yeast phospholipids using one-dimensional thin-layer chromatography was adapted from a protocol by Vaden et al. [48]. First, silica gel TLC plates were prewashed in a CHCl_3 /MeOH (1:1) solution. Plates were wetted in 1.8 % boric acid in ethanol (w/w), dried for 5 min and baked for 15 min at 100 °C. Twenty μl of lipid samples as well as 10 μl of standards for PS, PC, PE (1.2 mg/ml each) and PI (2.5 mg/ml) were spotted onto the plates. The chromatography tank was equilibrated with the solvent CHCl_3 /EtOH/ H_2O /triethylamine (30:35:7:35) for at least 2 h. The TLC migrated for approximately 2 h before plates were dried. Staining of phospholipids was performed with ceric ammonium molybdate (provided by the laboratory of Günther Daum, Graz University of Technology), treated with H_2SO_4 and baked at 100 °C.

2.2.4 Protein expression in *P. pastoris*

2.2.4.1 Cell cultivation of *P. pastoris*

Small scale cultivation:

Single colonies of *P. pastoris* transformants were inoculated in 25 ml BMGY medium in 300 ml Erlenmeyer flasks with baffles. The cells were grown at 28 °C and 120 rpm until stationary phase and then induced by adding 25 ml of 1 % BMMY medium to obtain a final methanol concentration of 0.5 %. Induction was continued daily in the morning and in the evening over 3 days. Therefore, 2.5 ml of 10 % BMMY medium were added to maintain a methanol concentration of 0.5 %. One ml samples were taken after 0 h, 8 h, 24 h, 48 h and 72 h and stored at -20 °C.

Large scale cultivation:

Single colonies of *P. pastoris* transformants were inoculated in 100 ml BMGY medium in 2 L Erlenmeyer flasks with baffles. The cells were grown 28 °C and 120 rpm for 48 h until stationary phase and then induced by adding 100 ml of 2 % BMMY medium to obtain a final methanol concentration of 1 %. Induction was continued twice a day over 72 h by adding 2 ml of MeOH. Cells were harvested after 8 h or 72 h of induction as described in section 2.2.4.3.

2.2.4.2 Cell harvest and glass bead-disruption

One ml of the samples was centrifuged for 1 min at 4500 x *g* and 4 °C and the supernatant was discarded. The pellets were kept on ice. Two-hundred µl of ice-cold Breaking Buffer and an equal volume of glass-beads (size 0.5 mm) were added. The cells were disrupted in 8 subsequent 30 s vortexing and cooling steps. The cell debris was centrifuged at 2300 x *g* for 10 min at 4 °C and the clear supernatant containing the total cell lysate was transferred to a fresh microcentrifuge tube. Samples were stored at -20 °C until use.

2.2.4.3 Merckenschlager cell disruption and membrane preparation

All centrifugation steps were carried out at 4 °C and samples were kept on ice. Two hundred ml cell cultures from large-scale cultivations were collected by centrifugation for 5 min at 3000 x *g* and washed with dH₂O before they were again centrifuged for 5 min at 3000 x *g*. The cell wet weight (CWW) was determined and yielded amounts between 4 g and 10 g. The pellets were resuspended in 1 ml TE-buffer per 1 g of CWW together with 2 µl PMSF per 1 g

of CWW. Disruption was performed with a Merckenschlager homogenizer under CO₂ cooling for 3 min with 30 s cooling intervals. Unbroken cells and glass beads were removed by centrifugation at 3000 x *g* for 10 min. Differential centrifugation steps were performed as shown in Figure 10. The cell lysate was centrifuged at 12,000 x *g* for 15 min to obtain supernatant S12 and pellet P12 fraction. Supernatant S12 was spun at 20,000 x *g* for 15 min to receive supernatant S20 and pellet P20. Ultracentrifugation of supernatant S20 at 100,000 x *g* for 45 min yielded the fractions S100 and P100. The pellets were resuspended in 10 mM Tris-HCl buffer, pH 7.4 and all aliquots taken from every fraction were frozen at -80 °C until use.

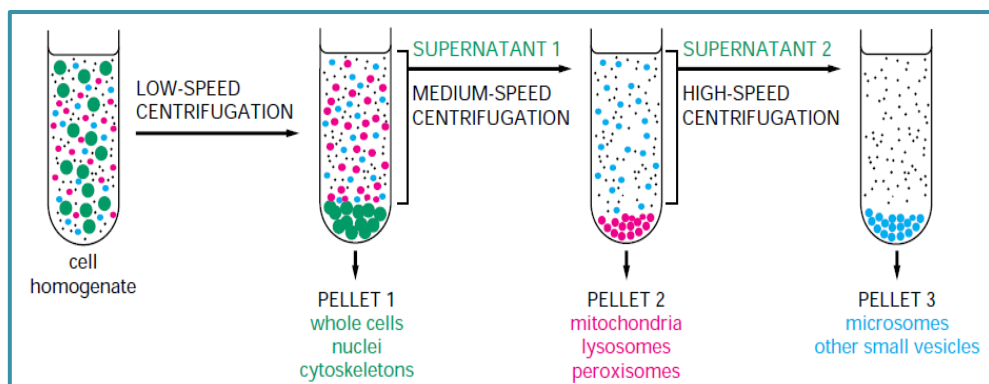


Figure 10. Differential centrifugation. Repeated centrifugation at progressively higher speeds was used to achieve fractionation of cell homogenates. Image was taken from Alberts et al. [49].

2.2.4.4 Protein Quantification by the method of Lowry

Protein concentrations were determined using the method of Lowry [50]. For generating the calibration curve, different dilutions of BSA (0.125 mg/ml, 0.25 mg/ml, 0.5 mg/ml, 1 mg/ml and 2 mg/ml) were used. Protein samples were diluted 1:10 except for the S100 fraction. Twenty five µl of the sample were added to 400 µl H₂O. Proteins were then precipitated with 100 µl of 50 % TCA prior to quantification as described in section 2.2.4.5 to get rid of disturbing components. The pellets were dissolved in 100 µl of Solution C for 30 min at 65 °C. For quantification, 100 µl of the samples were added to 300 µl of H₂O in a test tube and 2 ml of Solution A were added, followed by 10 min incubation at RT. After adding 200 µl of Solution B, samples were again incubated for 30 min at RT and absorption was measured spectrophotometrically at 546 nm. Protein amounts were calculated using the equation from the BSA calibration curve (Figure 19).

Example for the calculation:

The sample was diluted 1:10 and 25 μl were TCA precipitated. The Absorption at 546 nm was 0.2847. Equation from calibration curve:

$$y = -6 \cdot 10^{-6}x^2 + 0.0052x + 0.0154 \quad (\text{Equation 2})$$

Resolving Equation 2 for x by inserting 0.2847 for y gives **55.3 $\mu\text{g}/\mu\text{l}$** . The dilution factor and the amount precipitated also had to be considered in Equation 3:

$$\frac{55.3 \mu\text{g}}{25 \mu\text{l}} * 10 = 22.12 \mu\text{g}/\mu\text{l} \quad (\text{Equation 3})$$

From the protein amount (**22.12 $\mu\text{g}/\mu\text{l}$**), the μl needed for precipitation of 50 μg protein could be calculated as shown in Equation 4:

$$\frac{50 \mu\text{g}}{22.12 \mu\text{g}/\mu\text{l}} = 2.26 \mu\text{l} \quad (\text{Equation 4})$$

Therefore, **2.26 μl** were used for protein precipitation.

2.2.4.5 TCA precipitation

For protein precipitation, 400 μl of H_2O were placed in a microcentrifuge tube. The amount representing 50 μg of protein was added to the water. Then, 100 μl of ice-cold 50 % TCA was added, vortexed briefly and incubated for at least 1 h on ice to precipitate the proteins. The proteins were pelleted for 10 min at 16,100 x g and 4 °C. Supernatants were discarded and the pellets were washed with 500 μl of ice-cold water. The centrifugation step was repeated for 5 min at 16,100 x g and the supernatants were again discarded. The pellets were resuspended in 25 μl SDS sample buffer. Proteins were denatured for 30 min at 45 °C instead of the common 95 °C to avoid aggregation.

2.2.4.6 SDS-PAGE

SDS-PAGE was performed with self-made 12.5 % SDS-gels. After pouring the resolving gel, it was covered with 700 μ l of n-butanol and polymerized for about 1 h. Then, the stacking gel was poured, polymerized for approximately 30 min and stored at 4 °C until use. The volumes for the resolving and the stacking gels are calculated for pouring five gels (Table 10). For SDS-PAGE, 10 μ l of the sample were loaded on the gel, corresponding to 20 μ g protein. Five μ l of the standard PageRuler™ Prestained Protein Ladder were used to compare the size of the protein (Fig. 9). The chamber was filled with 1 x SDS running buffer. The running conditions for electrophoresis were 35 mA per gel, max. voltage and max. power for 60 to 90 min.

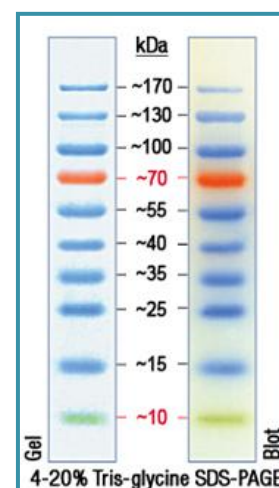


Figure 9. PageRuler™ Prestained Protein Ladder used for SDS-PAGE.

TABLE 10. Composition of self-made SDS-PAGE gels.

Resolving gel (12.5 %)		Stacking gel (3 %)	
Acrylamid/Bis 30 %	11.25 ml	Acrylamid/Bis 30%	2.45 ml
Tris-HCl buffer, 1.5 M, pH 8.8	10.5 ml	Tris-HCl buffer, 0.5 M, pH 6.8	2.45 ml
SDS 10% (w/v)	281.25 μ l	SDS 10% (w/v)	187.5 μ l
dH ₂ O	6 ml	dH ₂ O	13.9 ml
TEMED	28.13 μ l	TEMED	18.75 μ l
10 % APS (w/v)	140.63 μ l	10 % APS (w/v)	93.75 μ l

2.2.4.7 Western blot and immunodetection

The SDS gel was blotted onto a nitrocellulose membrane with the XCell II™ Blot Module. For this purpose, the sandwich was built up as shown in Figure 10. The inner chamber was filled with 1 x transfer buffer and the outer chamber was filled with water and ice for cooling. Blotting was performed at 25 V, 160 mA, 25 W for 1 h. After blotting, the membrane was stained with Ponceau S to see whether the transfer was successful. Destaining was performed with H₂O.

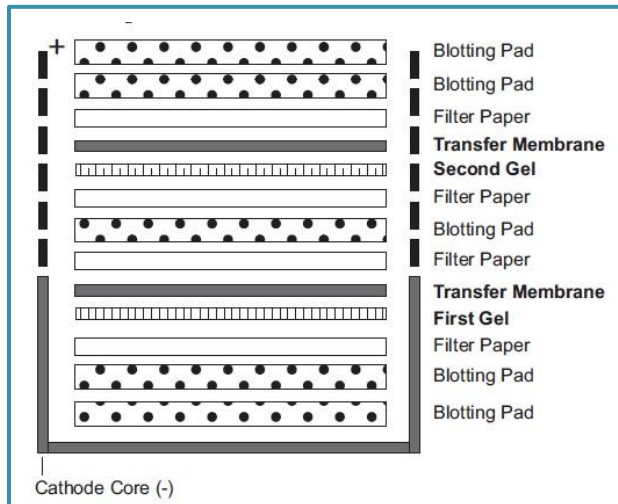


Figure 10. Setup of Western blot sandwich using the XCell II™ Blot Module from Invitrogen to blot two membranes at the same time

detection. An antibody against yeast plasma membrane H^+ -ATPase (Pma1p) produced in rabbit was used as marker for plasma membrane localization. Further antibodies used as marker for ER localization (Wbp1p, Sec61p, Kar2p) and for mitochondrial localization (Por1p) were also tested. These primary antibodies were diluted 1:1000 and were provided by Günther Daum (Institute of Biochemistry, Graz University of Technology).

Washing of the membrane after incubation of the primary antibody was performed 3 times with 1 x TBST buffer for 5 min at moderate shaking. The secondary antibody, a horseradish peroxidase conjugated anti-rabbit IgG, was diluted 1:5000 for the best results and incubated for 1 h at room temperature with moderate shaking. The membrane was washed again and then incubated for 10 min with the detection solution “SuperSignal® West Pico Chemiluminescent Substrate Kit”. The enhancer solution and the peroxide solution were mixed in a 1:1 ratio before use and were protected from light. The chemiluminescent signal was then captured with the G:BOX Bioimaging System.

2.2.5 Activity assays

2.2.5.1 Cytochrome c reductase assay

The Cytochrome c reductase assay was performed on the different membrane fractions of *P. pastoris* WT and cholesterol strain. The assay was used to detect the ER in the membrane fractions by measuring specifically the NADPH-dependant Cytochrome c reductase activity,

For immunodetection, the membrane had to be blocked with TBST-milk for at least 1 h at RT. The membrane was rinsed with 1 x TBST buffer and incubated with the primary antibody over night at 4 °C with moderate shaking. Primary antibodies against $\alpha 3$ (rabbit anti-KETYY) and $\beta 1$ (rabbit anti-GERK) subunits were kindly donated by Steven J. D. Karlish (Weizmann Institute, Israel). Several dilutions were tested, as it turned out that 1:500 was working best for the

which is localized in the ER. The assay setup was based on the “Cytochrome c Reductase (NADPH) Assay Kit” from Sigma-Aldrich.

Prior to measurements, the samples were diluted 1:10 in enzyme dilution buffer. The working solution had to be prepared freshly by dissolving 9 mg Cytochrome c in 20 ml Cyt-c reductase assay buffer to yield a final concentration of 36 μM . The NADPH working solution was also prepared freshly by mixing 22 μl of NADPH stock solution with 1 ml H_2O . This solution was stable for 2 h at RT. 50 μl of enzyme dilution buffer were used as Blank. The absorption was measured at 550 nm and 25 °C with a spectrophotometer set to the kinetic mode with parameters set to 5 s initial delay, 10 s interval and 7 readings.

Assay setup in cuvettes:

950 μl working solution
 30 μl Sample (diluted 1:10 in Enzyme Dilution Buffer)
 20 μl Cyt-c oxidase inhibitor solution
100 μl NADPH (was added last to start the reaction)
 1.1 ml total volume

Calculation of enzyme activity:

One unit will reduce 1.0 μmol of oxidized cytochrome c in the presence of 100 μM NADPH per minute at pH 7.8 at 25 °C.

$$\text{Units/ml} = \frac{\Delta A_{550}/\text{min} \times \text{dil} \times 1.1}{21.1 \times \text{Enzvol}} \quad (\text{Equation 5})$$

$\Delta A_{550}/\text{min} = \Delta A_{\text{sample}} - \Delta A_{\text{blank}} = \text{slope of the line}$

$\text{dil} = \text{the dilution factor of the original enzyme sample}$

$\text{Enzvol} = \text{volume of the enzyme sample (ml)}$

$21.1 = \text{extinction coefficient } (\epsilon^{\text{mM}}) \text{ for reduced cytochrome c}$

$1.1 = \text{reaction volume (ml)}$

For example, if $\Delta A_{550}/\text{min} = 0.0053$:

$$\text{Units/ml} = \frac{0.0053 \times 10 \times 1.1}{21.1 \times 0.03} = 0.092 \text{ U/ml} \quad (\text{Equation 6})$$

The activity was then calculated corresponding to the protein amount in the samples, hence the activity is given in U/ μg .

2.2.5.2 Na,K-ATPase activity assay

Na,K-ATPase activity was basically determined as described by Kapri-Pardes et al. [51] with minor modifications. Crude membrane fractions were diluted 1:500 in TE-buffer and 50 μl were added to 400 μl reaction mix containing 130 mM NaCl, 20 mM KCl, 3 mM MgCl_2 , 1 mM EDTA and 25 mM histidine, pH 7.4, in the presence or absence of 10 mM ouabain. To start the reaction, ATP was added freshly to 0.1 mM and the mixture was incubated at 37 $^\circ\text{C}$ for 15 min and 350 rpm. One hundred μl of each sample were transferred to 96-well plates and the released P_i was detected with “ P_i Color Lock Gold” Kit according to the manual. Absorbance of the green malachite dye complex which was formed by the release of inorganic phosphate due to ATP hydrolysis was measured at 635 nm (see Figure 12A, B). TE-buffer was used as blank and was subtracted from measured values. Specific Na,K-ATPase activity was defined as ATPase activity susceptible to inhibition by ouabain and was calculated as the difference in ATP hydrolysis with and without 10 mM ouabain in the assay.

The P_i calibration curve was generated by dilution of 0.1 mM P_i standard, which was delivered with the Kit. The concentrations ranged from 0 μM to 50 μM of P_i and samples were measured in triplicate at 635 nm as described in the manual of the Kit.

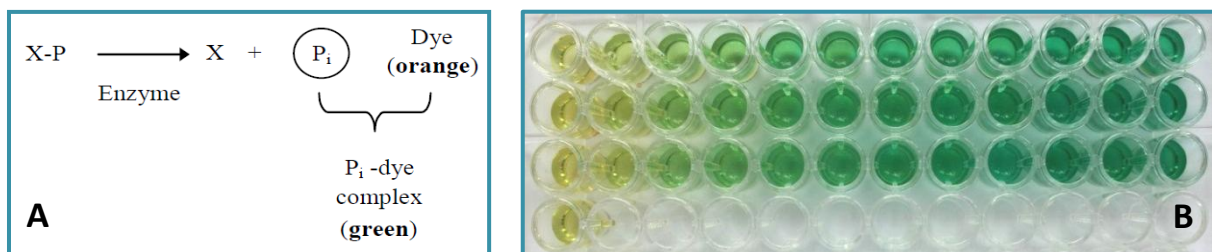


Figure 12. Detection of inorganic Phosphate using the “ P_i Color Lock Gold” Kit. (A) Reaction scheme of color formation. (B) Color development of the green malachite dye complex.

Example for the calculation of Na,K-ATPase activity:

First, the actual protein amount present in the assay volume had to be determined. For instance, the protein amount of a sample was 28.13 $\mu\text{g}/\mu\text{l}$. It was diluted 1:500 to 0.05626 $\mu\text{g}/\mu\text{l}$ and 50 μl of the diluted enzyme were added to 400 μl reaction medium, yielding a protein amount of 2.813 μg in 450 μl . Therefore, the effective concentration in the assay was **6.25 mg/l**.

After performing the assay, an absorbance of 0.2135 at 635 nm was measured.

Equation from calibration curve:

$$y = 0.0183 x \quad (\text{Equation 7})$$

Resolving Equation 7 for x by inserting 0.2135 for y gives **11.67 μM P_i** . This value had to be corrected for the effective protein amount present in the sample:

$$\frac{11.67 \mu\text{mol/l}}{6.25 \text{ mg/l}} = 1.87 \mu\text{mol } P_i/\text{mg protein}/15 \text{ min} \quad (\text{Equation 8})$$

The activity was therefore **7.48 $\mu\text{mol } P_i/\text{mg protein/h}$** .

2.2.6 Radioligand binding studies

2.2.6.1 Cell counting with the Neubauer improved counting chamber

P. pastoris cells were cultivated as described in section 2.2.4.1 for 8 h and 72 h, respectively. Samples were diluted 1:100 (8 h) or 1:1000 (72 h) in BMGY and 10 – 20 μl were placed on the counting chamber. Diagonals were counted microscopically using the Neubauer improved counting chamber (see Figure 11A, B).

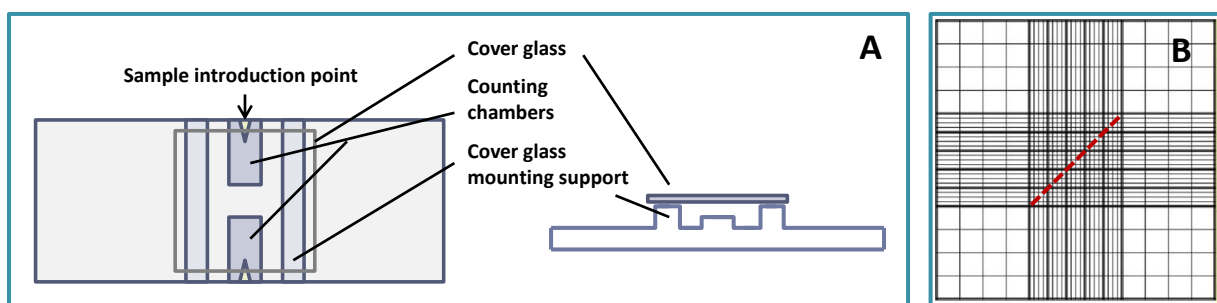


Figure 11. Neubauer improved counting chamber. (A) Sample introduction and assembling of the chamber. (B) The red dashed line indicates the diagonal squares used for cell counting.

For determining the cell number, the mean value was calculated from the five diagonal fields and cells/ml were determined using Equation 9.

$$\frac{\emptyset \text{ cells} \times \text{dil}}{4 \times 10^{-6}} = \text{cells/ml} \quad (\text{Equation 9})$$

\emptyset cells = mean value of cells counted from 5 diagonals

dil = dilution factor

4×10^{-6} = dimension of squares ($0.04 \text{ mm}^2 \times 0.1 \text{ mm} = 0.004 \text{ mm}^3 = 4 \times 10^{-6} \text{ cm} = 4 \times 10^{-6} \text{ ml}$)

TABLE 11. Cell counting after 8 h of methanol induction

P. p. WT	Cells counted					\emptyset	Cells/ml	OD ₆₀₀	ml needed for 1×10^9 cells
	25	28	20	29	30	26.4			
22	28	26	26	32	26.8				
P. p. WT + ATPase	Cells counted					\emptyset	Cells/ml	OD ₆₀₀	ml needed for 1×10^9 cells
	32	42	42	38	41	39			
38	32	30	38	33	34.2				
P. p. Chol.	Cells counted					\emptyset	Cells/ml	OD ₆₀₀	ml needed for 1×10^9 cells
	28	23	31	34	29	29			
22	18	35	32	31	27.6				
P. p. Chol. + ATPase	Cells counted					\emptyset	Cells/ml	OD ₆₀₀	ml needed for 1×10^9 cells
	17	19	9	12	11	13.6			
12	20	20	16	14	16.4				
P. p. SMD1168+ ATPase	Cells counted					\emptyset	Cells/ml	OD ₆₀₀	ml needed for 1×10^9 cells
	32	42	27	54	40	39			
32	40	42	45	32	38.2				
P. p. S- α 3 β 1	Cells counted					\emptyset	Cells/ml	OD ₆₀₀	ml needed for 1×10^9 cells
	42	41	37	45	23	37.6			
37	41	44	39	34	39				

TABLE 12. Cell counting after 72 h of methanol induction

P. p. WT	Cells counted					\emptyset	Cells/ml	OD ₆₀₀	μ l needed for 1×10^9 cells
	4	8	9	8	7	7.2			
4	7	7	3	6	5.4				
P. p. WT + ATPase	Cells counted					\emptyset	Cells/ml	OD ₆₀₀	μ l needed for 1×10^9 cells
	5	14	5	5	12	8.2			
6	8	10	13	3	8				

P. p. Chol.	Cells counted						\emptyset	Cells/ml	OD₆₀₀	μl needed for 1 x 10⁹ cells
	7	1	5	10	8	6.2	1.6 x 10 ⁹	51.4	625 μ l	
	14	8	7	0	4	6.6				
P. p. Chol. + ATPase	Cells counted						\emptyset	Cells/ml	OD₆₀₀	ml needed for 1 x 10⁹ cells
	4	3	6	5	2	4	7.5 x 10 ⁸	36.6	1.333 ml	
	8	1	4	4	3	2				
P. p. SMD1168+ ATPase	Cells counted						\emptyset	Cells/ml	OD₆₀₀	μl needed for 1 x 10⁹ cells
	6	3	4	8	8	5.8	1.3 x 10 ⁹	51.6	769.2 μ l	
	5	1	8	5	4	4.6				
P. p. S-α3β1	Cells counted						\emptyset	Cells/ml	OD₆₀₀	μl needed for 1 x 10⁹ cells
	3	8	4	10	5	6	1.75 x 10 ⁹	49.3	571.4 μ l	
	10	6	8	10	6	8				

2.2.6.2 Binding of [³H]-ouabain to intact cells

To estimate the amount of Na,K-ATPase proteins present on the surface and, therefore, in the plasma membrane, radioactively labeled ouabain was used as tracer due to its ability to bind specifically to the membrane protein at the outside of the cell. To ensure effective binding of ouabain, sodium orthovanadate had to be added to the reaction. Sodium orthovanadate is a potent inhibitor for dephosphorylation and had itself to be activated before binding specifically to Na,K-ATPase in its phosphorylated state. By activation, the Na₃VO₄ is depolymerized and turns into a more potent inhibitor of phosphatases [52]. This step was necessary to ensure that the [³H]-ouabain could bind with high affinity to Na,K-ATPase, as it is known that ouabain binding affinity is enhanced in the phosphorylated state of the protein [21, 51].

A 200 mM stock solution of sodium orthovanadate was prepared by dissolving 735.64 mg Na₃VO₄ in approximately 15 ml H₂O. The pH was adjusted to 10 with NaOH or HCl, resulting in a yellow color development. The solution was boiled for approximately 10 min until it became colorless again. After cooling to RT, these steps were repeated until the solution remained colorless and the pH was stable. Finally, the volume was adjusted to 20 ml with H₂O. Aliquots of the solution were stored at – 20 °C. Before use, aliquots were heated shortly at 90 °C – 100 °C and vortexed to redissolve crystals.

Saturation binding of [³H]-ouabain to whole cells was basically performed according to the protocols of Pedersen et al. [22] and Reina et al. [24]. First, the 26 μM [³H]-ouabain (38.4 Ci/mmol) was diluted with cold ouabain. Therefore, a 52 μM solution of cold ouabain dissolved in EtOH was prepared and 100 μl of 52 μM cold ouabain were mixed with 100 μl of 26 μM [³H]-ouabain to obtain a 39 μM [³H]-ouabain solution with a specific activity of 13 Ci/mmol.

Samples containing 1×10^9 cells were collected by centrifugation for 5 min at 1000 x g and 4 °C. Pellets were then resuspended in 1 ml Binding Buffer containing various concentrations (500 nM, 80 nM and 10 nM) of labeled ouabain. The cells were incubated for 90 min at 37 °C and 1000 rpm and kept on ice for another 30 min. To estimate non-specific binding, samples were incubated with 500 nM [³H]-ouabain together with 1 mM cold ouabain. Unbound [³H]-ouabain was removed by centrifugation for 5 min at 1000 x g at 4 °C and pellets were washed twice with ice-cold water before they were resuspended in 100 μl H₂O. Samples were transferred to scintillation vials and 8 ml of Ultima-Gold scintillation cocktail were added. Vigorous vortexing was necessary to ensure distribution of cell material in the viscous scintillation cocktail. Samples were incubated for 30 min at RT, before the bound [³H]-ouabain was measured with the Liquid Scintillation Analyzer (see Figure 12). The total number of binding sites on the cell surface (B_{\max}) was determined after 72 h of induction by plotting the data obtained according to Scatchard method [54]. The maximal binding sites per cell B_{\max} could be calculated from the intercept with the x-axis.

Example for the calculation:

The intercept with the x-axis was calculated using the regression line fitted to the data points. For the cholesterol strain, Equation 10 was used.

$$y = -0.0034 x + 0.002 \quad (\text{Equation 10})$$

For $y = 0$, the intercept was 0.7941 nM/ml \triangleq 0.794 pmol \triangleq **0.794 x 10⁻¹² mol**. As 1 mol contains 6.022×10^{23} molecules and 1×10^9 cells were incubated, the number of binding sites per cell could be calculated:

$$B_{max} = \frac{4.78 \times 10^{11} \text{ molecules}}{1 \times 10^9 \text{ cells}} = 478 \text{ binding sites/cell} \quad (\text{Equation 11})$$

K_d was calculated from the slope from Equation 10:

$$K_d = -\frac{1}{k} = -\frac{1}{-0.0034} = 294.1 \text{ nM} \quad (\text{Equation 12})$$

Therefore, the affinity for ouabain binding was $294.1 \text{ nM} \triangleq 2.941 \times 10^{-7} \text{ M}$.



Figure 12. Liquid Scintillation Analyzer Tri-Carb2900TR.

Samples were counted according to protocol #6 using QuantaSmart™ Software with following setup: Assay Type = CPM; Nuclide = ^3H ; Quench indicator = tSIE/AEC; Count time = 4 min. The picture was taken from perkinelmer.com.

2.2.7 Immunofluorescence

Immunofluorescence experiments were performed by Tamara Wriessnegger.

2.2.7.1 Fixation and permeabilization of cells

P. pastoris strains were grown in BMGY and induced with methanol for 8 h and 72 h respectively. Cells were counted with the Neubauer Improved hemocytometer as described in section 2.2.6.1 and 1×10^8 cells were harvested by centrifugation. Samples were then resuspended in 200 μl of 37 % aqueous formaldehyde and incubated for 30 min at 28 °C before spinning for 5 min at 600 x *g*. The first washing step was done with 100 mM KPi buffer, pH 7.5. Afterwards, 100 mM KPi buffer containing 4 % formaldehyde was added and the second washing step was done with solution B. Pellets were resuspended in solution B with 20 μl of Zymolyase (5 mg/ml) followed by incubation at 28 °C for 30 min with gentle shaking. Samples were centrifuged at 200 x *g* and washed once with 1 ml of solution C. The pellets were resuspended in 1 ml of solution C with 1 % SDS and washed again twice with solution C. The fixed and permeabilized cells were stored at 4 °C until use.

2.2.7.2 Preparation of multiwell slides for microscopy

Each well of the multiwell slides was coated with 10-20 μl of 0.1 % poly-L-lysine in H_2O and incubated for 10 min at RT. Poly-L-lysine was removed, slides were washed five times with H_2O and dried for 10 – 15 min. The fixed cells were resuspended in 500 μl of solution C and 20 μl were pipetted into the wells, incubated for 15 min and removed again. Twenty μl of Blocking solution was added, incubated for 30 min and removed again. Twenty μl of the primary rabbit Anti-KETYY or Anti-GERK antibodies (diluted 1:100 in PBS with albumin) were added and incubated over night at 4 °C. For removal of the primary antibody, wells were washed eight times with 20 μl PBS with albumin. Twenty μl of the secondary antibody (Goat anti-Rabbit IgG DyLight 488 conjugated; diluted 1:500 in PBS with albumin) were added and incubated for 60 min at RT in a humid chamber in the dark. The slide was washed five times with PBS Albumin and 3 μl Vectashield was added. Finally, the samples were covered with a cover slip (40 x 50 mm) and fixed with nail polish on both ends. The slides were stored at 4 °C.

3 Results

3.1 Growth studies of different *P. pastoris* strains

The growth behavior of the *P. pastoris* strains used in this work in BMGY media was initially studied and results are shown in Figure 13. While the *P. pastoris* WT, *P. pastoris* SMD1168 and *P. pastoris* DHCR7 strains show similar growth rates, it is seen that *P. pastoris* $\Delta erg5::DHCR7$ and *P. pastoris* $\Delta erg6::DHCR24$ mutants grow slower but still reach high cell densities. The cholesterol-producing strain has a specific growth rate of 0.11 h^{-1} , indicating that proliferation is much slower compared to the WT (0.25 h^{-1}) and SMD1168 (0.29 h^{-1}) strain. The intermediate *P. pastoris* $\Delta erg5::DHCR7$ also has a slightly reduced growth rate of 0.21 h^{-1} (Table 13). This points out that the altered sterol composition can affect cell physiology.

TABLE 13. Specific growth rates of different *P. pastoris* strains

Strain	Specific growth rate (μ)	OD ₆₀₀ after 36 h	OD ₆₀₀ after 56 h
<i>P. pastoris</i> WT	0.25 h^{-1}	60	n. d.
<i>P. pastoris</i> SMD1168	0.29 h^{-1}	63	n. d.
<i>P. pastoris</i> DHCR7	0.25 h^{-1}	69	n. d.
<i>P. pastoris</i> $\Delta erg5::DHCR7$	0.21 h^{-1}	47	60
<i>P. pastoris</i> $\Delta erg6::DHCR24$	0.17 h^{-1}	40	55
<i>P. pastoris</i> cholesterol strain	0.11 h^{-1}	4	32

n.d. = not determined

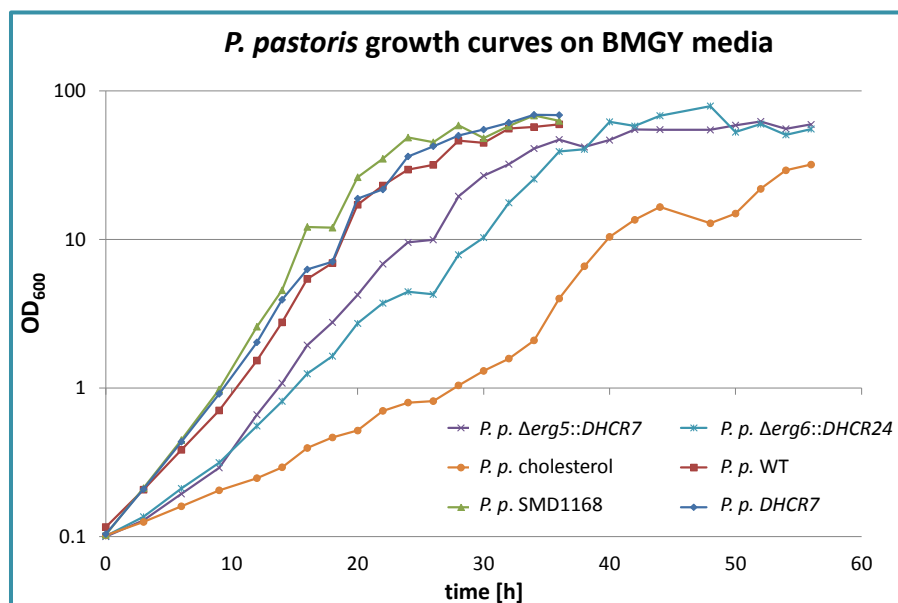


Figure 13. *P. pastoris* growth curves on BMGY media. Growth was monitored by measuring the OD₆₀₀ photometrically every 3 h in the early phase and every 2 h in the later exponential phase until cells reached stationary phase.

3.2 Construction of a *P. pastoris* $\Delta cho1$ knockout strain

3.2.1 Overlap extension PCR and sequencing of the *CHO1* knockout cassette

For the ongoing work, a *P. pastoris* strain deficient of producing phosphatidylserine should be created to be able to study the influence on heterologous Na,K-ATPase expression. In order to create a $\Delta cho1$ knockout strain that lacks phosphatidylserine synthase, a *CHO1* knockout cassette was created. The fragments for this cassette were generated with 3 independent PCRs, yielding the *CHO1* upstream fragment of 829 bp, the *CHO1* downstream fragment of 906 bp, as well as the *HPH* fragment of 1648 bp (Figure 14, A). The fragments were assembled using overlap extension PCR, resulting in the final product of a size of 3.3 kb (Figure 14, B). Several unspecific PCR artifacts emerged during the reaction, which were eliminated by gel purification. Figure 14, C shows the expression cassette ready for transformation into electrocompetent *P. pastoris* strains.

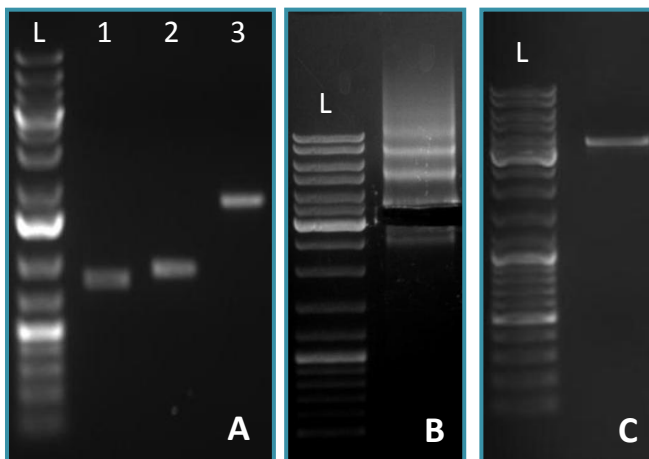


Figure 14. Construction of *CHO1* knockout cassette via overlap extension PCR. (A) Purified PCR fragments. 1: *CHO1* upstream fragment, 2: *CHO1* downstream fragment, 3: *HPH* fragment amplified from the pAG32-hph vector. L = GeneRuler™ 1 kb Plus DNA Ladder (B) Overlap extension PCR using all three fragments. (C) Final *cho1* knockout cassette after purification of the PCR fragment. L = GeneRuler™ DNA Ladder Mix.

Prior to transformation, the construct was sequenced to prove the absence of any unwanted mutations. Sequence Alignment was performed using Lasergene® SeqMan Pro™ (DNASTAR) Software and showed that the sequence was free of undesired mutations.

3.2.2 Transformation of *P. pastoris* WT and cPCR verification

Figure 15 shows the results of the Colony PCRs performed on the supposed *P. pastoris* $\Delta cho1$ transformants. The following primer pairs were used for colony PCR: Fw_cho1_genom and Rv_TEFpromoter as well as Fw_hph_marker and Rv_cho1_genom, which should yield products at 1387 bp and 1284 bp, respectively. Additional primers, FwHPH and RvHPH, were designed to bind directly in the *CHO1* gene sequence of the *P. pastoris* genome, which should yield no product if the gene was knocked out successfully. The colony PCR with the first two primer pairs were successful for transformants 1 – 3, where products of the desired sizes were obtained. Unfortunately every clone gave a PCR product with the third primer pair, indicating that the *CHO1* gene is still present in the genome of the strains, although the disruption cassette had been integrated correctly.

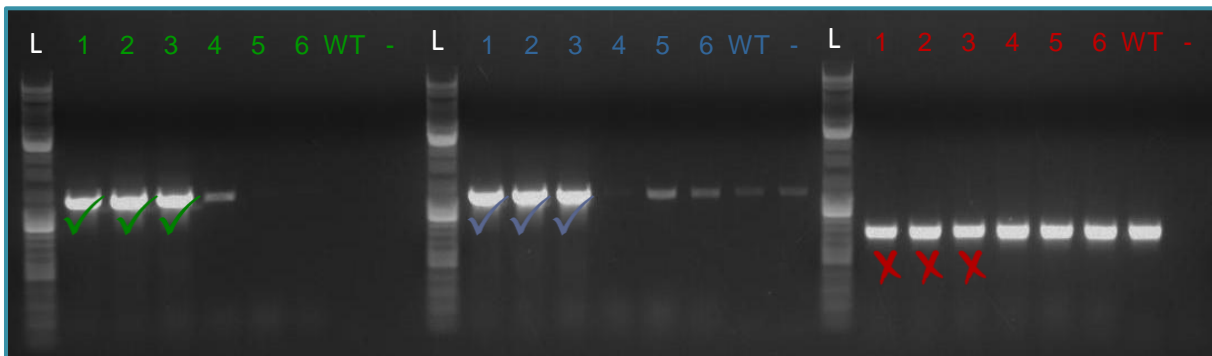


Figure 15. Colony PCR of different *P. pastoris* $\Delta cho1$ knockout mutants. Lanes 1 – 6 = Independent transformants of $\Delta cho1$ knockout cassette. (–) = n.t.c. L = GeneRuler™ DNA Ladder Mix. **Left:** PCR with the first primer pair binding at the *CHO1* upstream region and the TEF promoter (PCR product with 1387 bp expected). **Middle:** PCR with the second primer pair binding at the TEF terminator and the *CHO1* downstream region (PCR product with 1284 bp expected) **Right:** PCR with third primer pair binding inside the *CHO1* gene sequence (no PCR product expected at 781 bp).

3.2.3 Thin layer chromatography

To check if the cells were still able to produce phosphatidylserine, lipids were extracted and analyzed by thin layer chromatography (Figure 16). Seven independent clones were tested, but it can be seen that the lipid pattern were the same as in the WT. Therefore, PS is still present in the $\Delta cho1$ transformants and the knockout was not successful. Sample number 8 corresponds to a *S. cerevisiae* $\Delta cho1$ knockout mutant that was used as control. The analysis confirmed that no PS was produced by this strain. Nonetheless, overall lipid extraction did not work as well as for *P. pastoris* strains, resulting in a diminished signal on the TLC plates. Lipid standards were used to assign phospholipids, but seemingly the PE standard was not stained with this method.

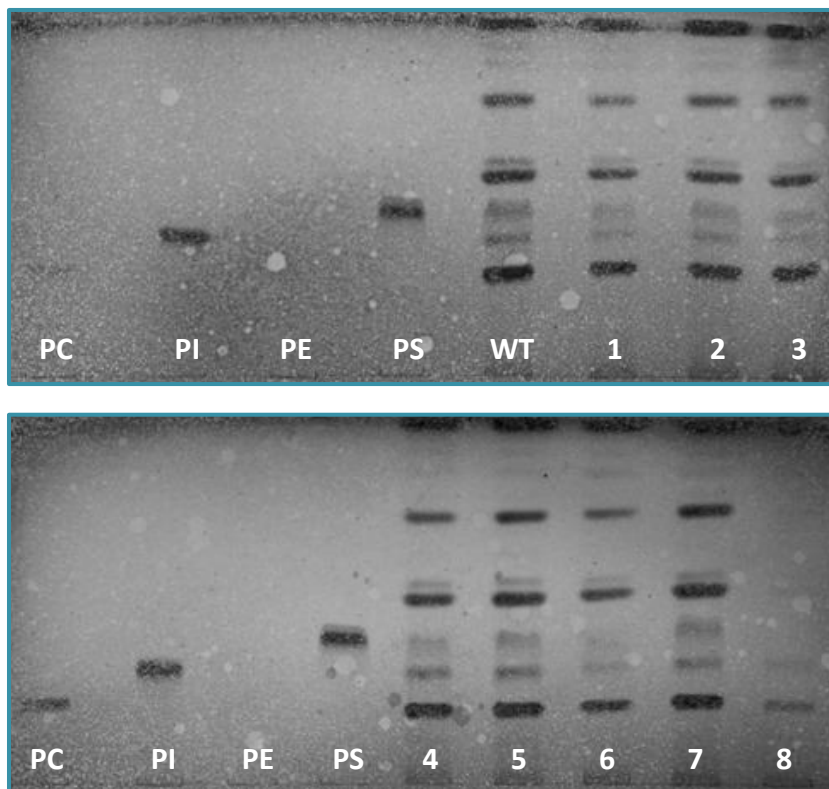


Figure 16. Thin-layer chromatography for analysis of *P. pastoris* phospholipids. CHCl_3 / EtOH / H_2O / Triethylamine was used as solvent and TLC plates were stained with ceric ammonium molybdate. **WT** = *P. pastoris* wildtype. **1–7** = putative *P. pastoris* $\Delta cho1$ knockout mutants. **8** = *S. cerevisiae* $\Delta cho1$ control strain. **PC, PI, PE, PS** = phospholipid standards.

3.3 Heterologous expression of Na,K-ATPase in different *P. pastoris* strains

The main part of this work was focused on the expression and characterization of Na,K-ATPase in different *P. pastoris* strains that have been changed in their membrane sterol composition. Special focus was thereby laid on the cholesterol-producing strain. The following sections show the results after transformation of the linearized pAO815- $\alpha 3\beta 1$ vector and the biochemical characterization of Na,K-ATPase $\alpha 3\beta 1$ expressed in selected strains.

3.3.1 Transformation of electrocompetent *P. pastoris* cells with pAO815- $\alpha 3\beta 1$

The vector pAO815- $\alpha 3\beta 1$ was linearized with *Bgl*II prior to transformation into *P. pastoris* cells to enhance integration into the genome via homologous recombination. The cut plasmid had a size of approximately 10.6 kb, which was not easy to distinguish from the uncut plasmid with 13 kb. However, the 2400 bp band showed that the plasmid had been digested and the corresponding band was cut out from the gel (Figure 17). After the vector was purified it was successfully transformed into *P. pastoris* strains.

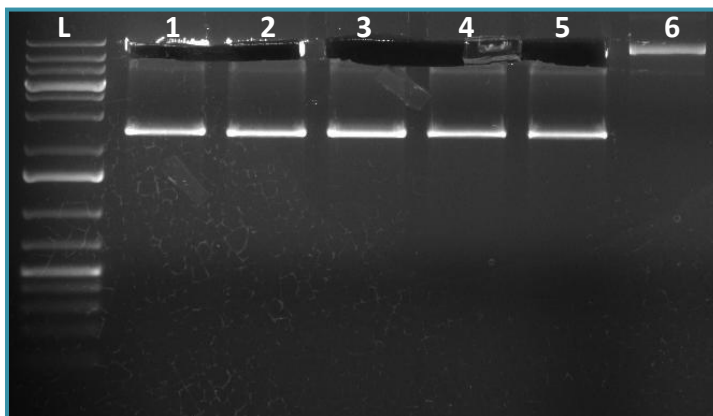


Figure 17. Plasmid pAO815 $\alpha 3\beta 1$ after linearization with *Bgl*II.

Lanes 1 – 5: plasmid cut with *Bgl*II
Lane 6: uncut plasmid. **L:** GeneRuler™ 1 kb Plus DNA Ladder. The lower bands represent the 2400 bp fragment that was cut out during *Bgl*II digestion.

3.3.2 Colony PCR verification

After transformation of the linearized plasmid into different *P. pastoris* strains, colonies appearing on the selective minimal media plates were again streaked out and tested with colony PCR. Figure 18 shows a representative agarose gel picture for typical colony PCR experiments conducted with positive transformants. The first primer pair yielded a PCR product of 1899 bp (Figure 18A), and the second primer pair gave a product of 1772 bp (Figure 18B). Transformants which gave PCR products of correct sizes with the two primer

pairs were selected for further cultivation steps. An overview of all positive transformants is given in Table 14.

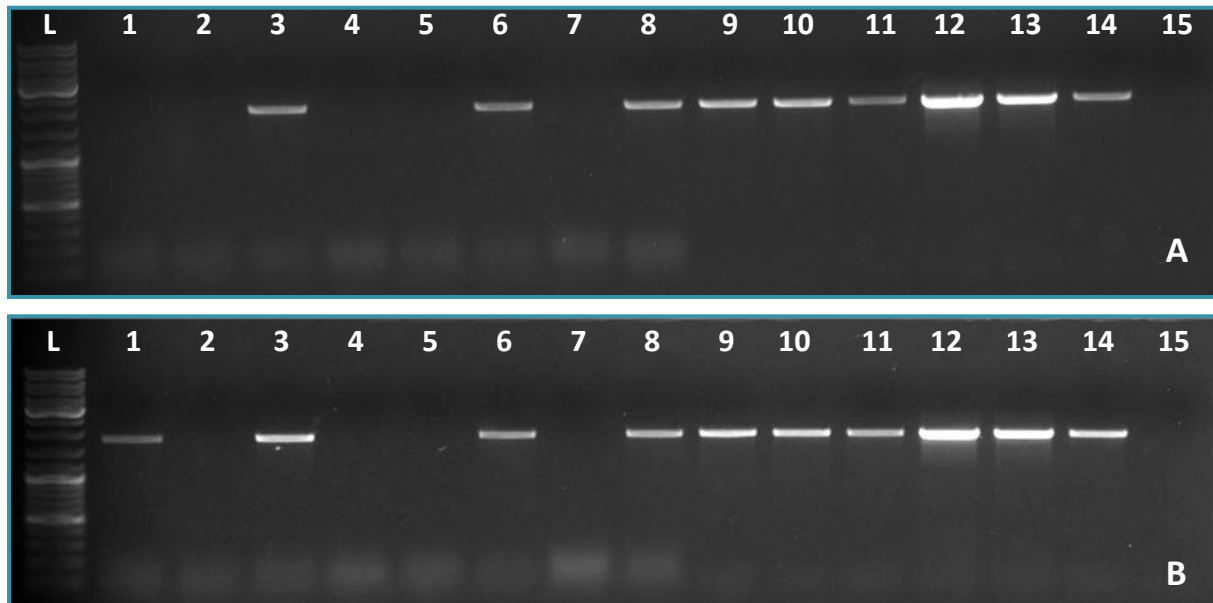


Figure 18. Colony PCR results after transformation of *P. pastoris* strains with pAO815- α 3 β 1 vector. (A) Fwd_AOXdown/Rev_alpha3 primer pair with corresponding PCR products of 1899 bp. (B) Fwd_alpha3/Rev_beta1 primer pair with corresponding PCR products of 1772 bp. Lanes 1 – 8: *P. pastoris* SMD1168[pAO815- α 3 β 1] transformants. Lanes 9 – 13: *P. pastoris* cholesterol strain[pAO815- α 3 β 1] transformants. Lane 14: Positive control. Lane 15: n.t.c. L: GeneRuler™ DNA Ladder Mix.

TABLE 14. Positive <i>P. pastoris</i> transformants containing Na,K-ATPase expression cassette				
Strain	Number		No. in strain collection ^c	
<i>P. pastoris</i> WT [pAO815 α 3/ β 1]	1		498	
	2 ^a		499	
	3		500	
<i>P. pastoris</i> Δ erg5::DHCR7 [pAO815 α 3/ β 1]	1		501	
	2 ^a		502	
	3 ^a		503	
	4		504	
	5		505	
<i>P. pastoris</i> DHCR7 [pAO815 α 3/ β 1]	1 ^a	5 ^b	506	510
	2 ^a	6 ^b	507	511
	3	7 ^b	508	512
	4	8 ^b	509	513
<i>P. pastoris</i> SMD1168 [pAO815 α 3/ β 1]	1 ^a		514	
	2		515	
	3		516	
	4		517	

	5	518
	6	519
<i>P. pastoris</i> Δerg6::DHCR24	1	520
[pAO815α3/β1]	2	521
	1 ^a	522
	2 ^a	523
<i>P. pastoris</i> cholesterol strain	3 ^a	524
[pAO815α3/β1]	4	525
	5	526
	1 ^b	527
	2	528
<i>P. pastoris</i> Δerg6	3 ^b	529
[pAO815α3/β1]	4	530
	5	531
	6	532

^a ... α3 subunit was detected with Western blot experiments

^b ... gave a weaker signal with colony PCR

^c ... strain collection of Harald Pichler

3.3.3 Cell harvest and protein quantification

After cultivation and methanol induction of selected *P. pastoris* strains containing the Na,K-ATPase expression cassette, samples were prepared as described in sections 2.2.4.3 and 2.2.4.4. To be able to calculate the precise protein amount used for Western blot experiments as well as for activity measurements, quantification was performed according to the Lowry method. The concentrations were calculated using the equation of the calibration curve (Figure 19). A complete table of calculated protein amounts of the samples can be found in Appendix A.

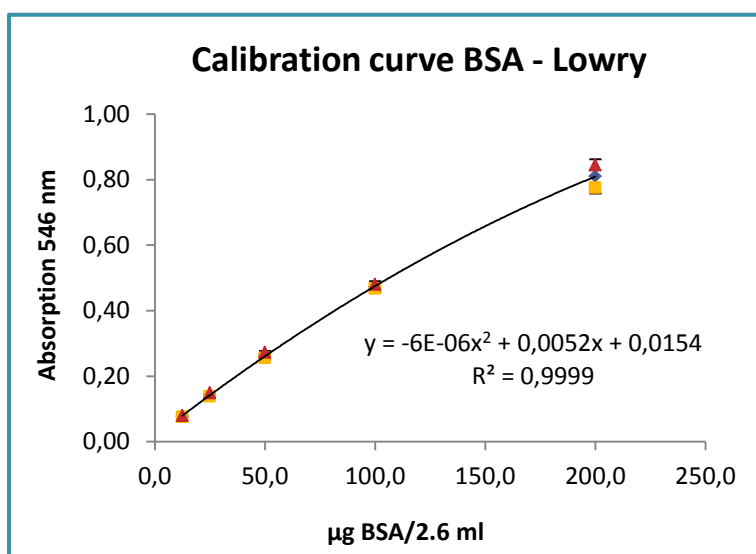


Figure 19. Calibration curve for protein quantification using the Lowry-method. Different dilutions of BSA (2 mg/ml) were used as standard and absorption was measured at 546 nm.

3.4 Western blot analysis

3.4.1 Detection of $\alpha 3$ subunit from total cell lysates

To examine Na,K-ATPase expression of the positive clones identified by colony PCR over different time points, samples from small-scale cultivations after 0 h, 8 h, 24 h, 48 h and 72 h of methanol induction were tested. Therefore, the $\alpha 3$ subunit was detected from the crude cell lysate without any purification or membrane fractionation steps (Figure 20 and Figure 21). Ponceau S staining was performed on every membrane after blotting to check for equal loading and a representative example picture is shown in Figure 20D.

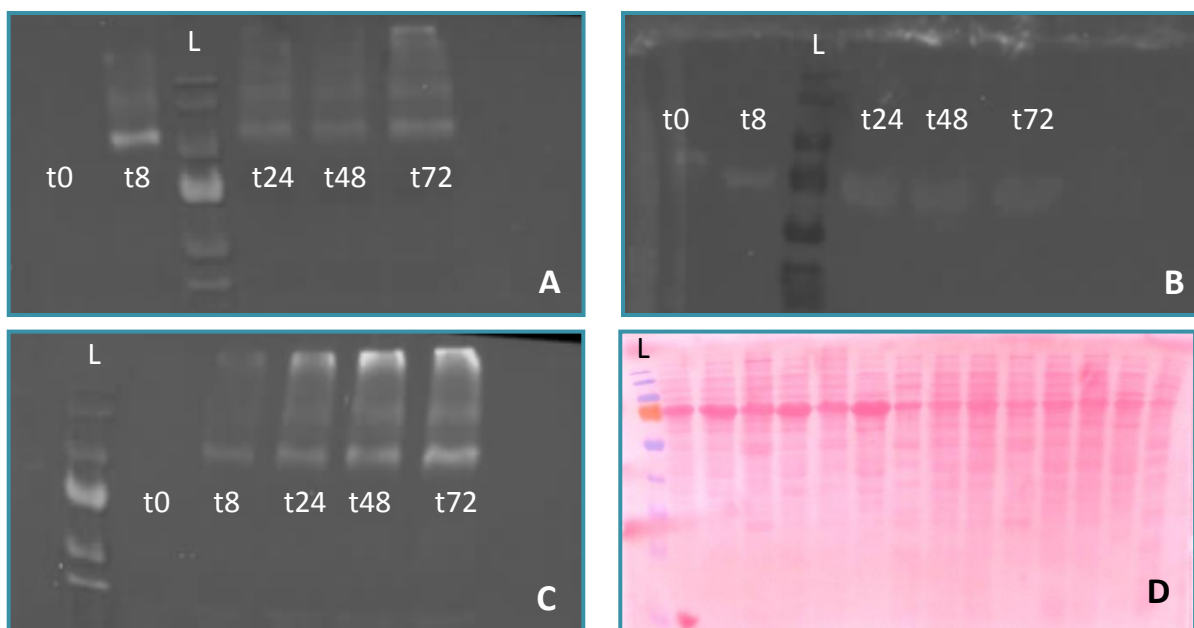


Figure 20. Western blot experiments. 20 μ g of protein were separated on a 12.5 % SDS gel by electrophoresis. (A) Total cell lysate from *P. pastoris* S- $\alpha 3\beta 1$, incubated with Anti-KETYY antibody against $\alpha 3$ subunit. (B) Total cell lysate from *P. pastoris* S- $\alpha 3\beta 1$, incubated with Anti-GERK against $\beta 1$ subunit, (C) Total cell lysate from *P. pastoris* cholesterol strain 1, incubated with Anti-KETYY against $\alpha 3$ subunit. (D) Example for a Ponceau-S stained membrane. L = Protein Ladder.

Panel A in Figure 20 shows that the positive control strain *P. pastoris* S- $\alpha 3\beta 1$ expressed Na,K-ATPase $\alpha 3$ subunit, but it was degraded with proceeding induction time. In the *P. pastoris* cholesterol strain 1, in contrast, the $\alpha 3$ subunit was expressed more stably even after 72 h (Figure 20C). The $\beta 1$ subunit was not detectable from the lysates. The faint bands seen at 70 kDa are not the appropriate size for the $\beta 1$ subunit and are therefore likely to be cross-reactive signals corresponding to AOX1p (Figure 20B). Proteins migrating at bigger apparent sizes than the expected 110 kDa for the $\alpha 3$ subunit were also seen for some samples. This

could be due to some proteins which were not denaturated completely. Also, the denaturation step could have been too rough, so that the proteins aggregated and built a larger complex.

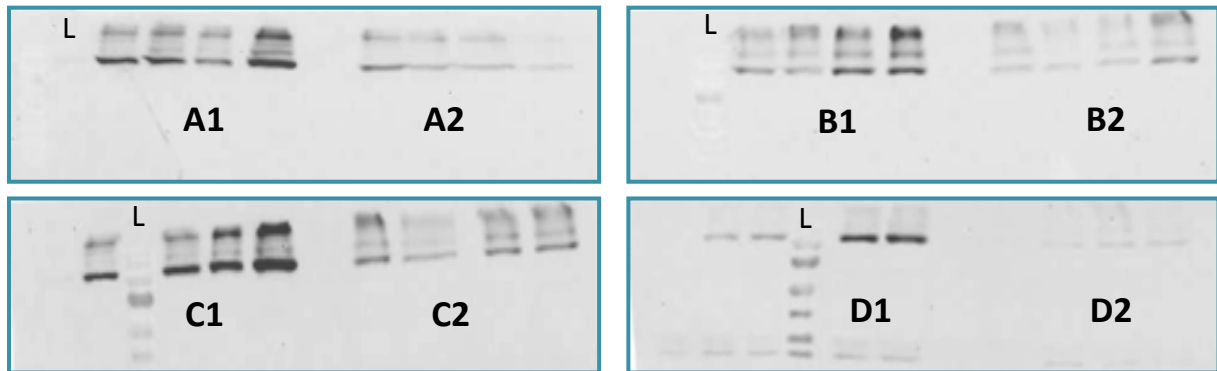


Figure 21. Western blot experiments of Na,K-ATPase expressing strains. 20 µg of protein were separated on a 12.5 % SDS gel by electrophoresis. All samples were detected with Anti-KETYY antibody against $\alpha 3$ subunit. (A1) *P. p.* WT 2, t0, t24, t48, t72 and t8. (A2) *P. p.* SMD1168 2, t0 – t72. (B1) *P. p.* DHCR7 1, t0 – t72. (B2) *P. p.* DHCR7 2, t0 – t72. (C1) *P. p.* $\Delta erg5::DHCR7$ 1, t0 – t72. (C2) *P. p.* $\Delta erg5::DHCR7$ 2, t0 – t72. (D1) *P. p.* cholesterol strain 2, t0 – t72. (D2) *P. p.* cholesterol strain 3, t0 – t72.

Figure 21 shows the results of the other *P. pastoris* strains that had been tested for time-dependant $\alpha 3$ -subunit expression. *P. pastoris* WT showed good expression levels after 8 h (Figure 21, A1), but also in this case the protein amount decreased over time. The same could be observed for the protease-deficient SMD1168 strain (Figure 21, A2). In strains which had an altered membrane sterol composition it was observed that the $\alpha 3$ -subunit was more stable with increasing induction time. This could be seen for the *P. pastoris* DHCR7 clones 1 and 2 (Figure 21, B1 and B2) as well as for the *P. pastoris* $\Delta erg5::DHCR7$ clones 1 and 2 (Figure 21, C1 and C2). Two further independent transformants of *P. pastoris* cholesterol strain were also tested (Figure 21, D1 and D2) and the result for clone 2 was comparable to clone 1. Clone 3, however, showed overall bad expression levels. Further work was continued with *P. pastoris* cholesterol strain No. 1.

3.4.2 Detection of $\alpha 3$ and $\beta 1$ subunits from membrane preparations

As the cholesterol strain was of particular interest for future experiments, the membrane fractions after methanol induction were studied in more detail for this strain. The sample number was reduced for this purpose and a closer look was taken onto Na,K-ATPase expressing *P. pastoris* cholesterol strain, *P. pastoris* SMD1168 strain, *P. pastoris* WT and *P. pastoris* S- $\alpha 3\beta 1$. Empty *P. pastoris* WT and *P. pastoris* cholesterol strains were also cultivated and used for control experiments.

Different centrifugation steps were conducted following cell harvest after 8 h and 72 h of methanol induction. The centrifugation steps yielded subfractions comprising the cell homogenate (H) at 1000 x g, the supernatant and pellet at 12,000 x g (S12, P12), the supernatant and pellet at 20,000 x g (S20, P20) and the supernatant and pellet after ultracentrifugation at 100,000 x g (S100, P100).

An antibody against yeast plasma membrane ATPase (Pma1p, 100 kDa) was used as plasma membrane marker for the particular fractions. As seen in Figure 22, the plasma membrane is traceable in smaller amounts in every fraction except S100, but occurs mainly in fractions P12, P20 and in the cholesterol strain also in P100. Figure 22 also shows that *P. pastoris* WT and *P. pastoris* cholesterol control cells, which had not been transformed with the pAO815- $\alpha 3/\beta 1$ vector, gave no signal in Western blot experiments.

After 8 h of induction, $\alpha 3$ subunit was expressed in all strains and also showed mainly co-localization with the plasma membrane (Figure 22, left panels). The major signals for $\alpha 3$, however, were detected in the P12 fraction, whereas the most intense band for Pma1p appeared in P20. The $\beta 1$ subunit is badly expressed after 8 h and is only visible as faint band in the P12 fraction in *P. pastoris* WT + ATPase, *P. pastoris* SMD1168 + ATPase and *P. pastoris* S- $\alpha 3\beta 1$ + ATPase strains. A small amount is also detectable in the P20 and P100 fractions in the *P. pastoris* cholesterol + ATPase strain.

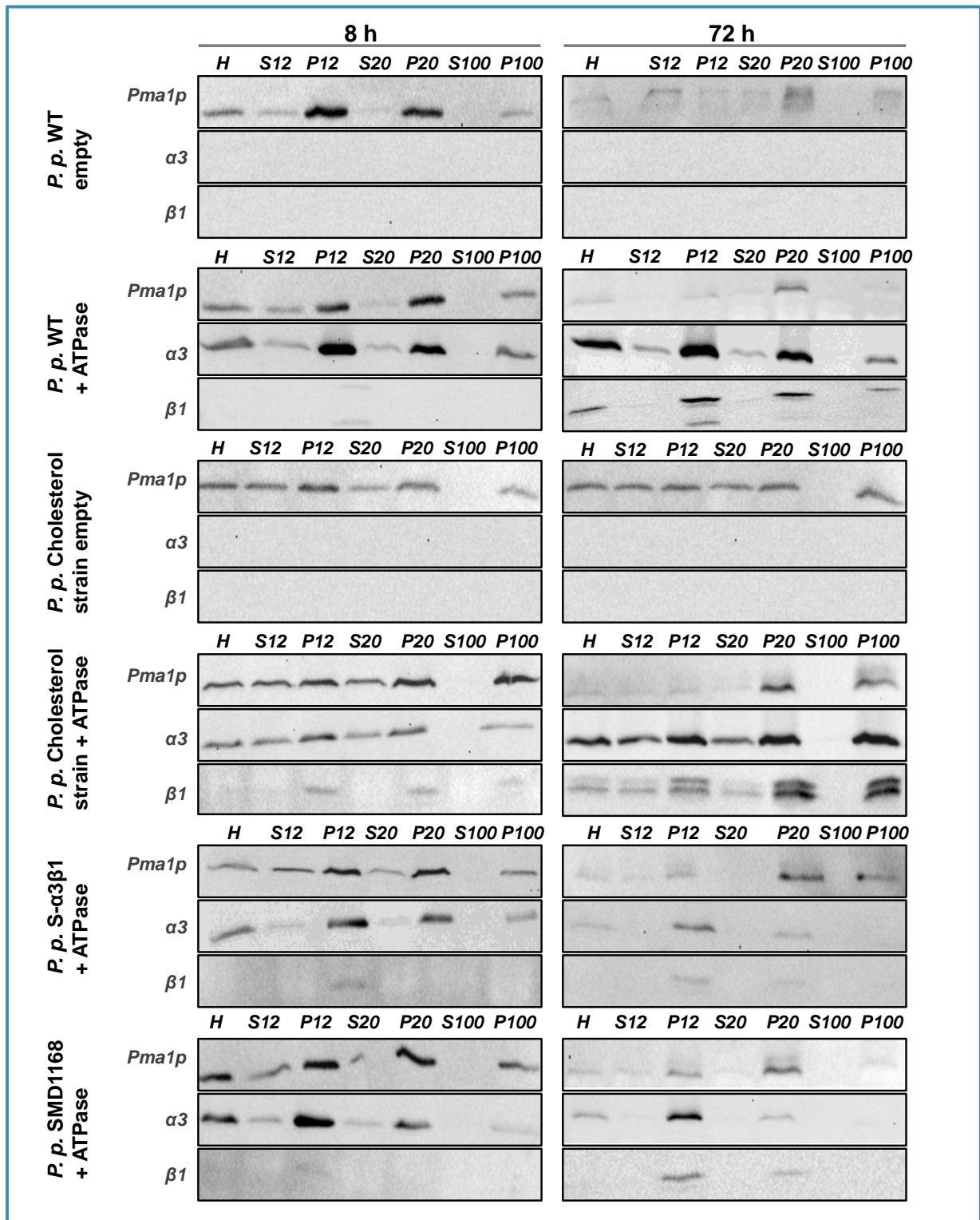


Figure 22. Western blot experiments with membrane fractions. *P. pastoris* cells were induced for 8 and 72 h, respectively. *P. pastoris* WT and *P. pastoris* cholesterol-producing strain without expression plasmid were treated the same way serving as negative control. After membrane fractionation, 20 μ g of total protein samples were separated on a 12.5 % SDS-PAGE gel and incubated with antibodies against subunits $\alpha 3$ (110 kDa), $\beta 1$ (44 kDa) and Pma1p (100 kDa). Different fractions after centrifugation are indicated in the lines as cell homogenate (H), supernatant and pellet at 12,000 x g (S12, P12), supernatant and pellet at 20,000 x g (S20, P20) and supernatant and pellet at 100,000 x g (S100, P100).

Interestingly, after 72 h of induction (Figure 22, right panels) the amount of expressed $\alpha 3$ subunit was decreased in the *P. pastoris* SMD1168 + ATPase and *P. pastoris* S- $\alpha 3\beta 1$ + ATPase strains, and it was not co-localized with Pma1p. Pma1p occurred mainly in fraction P20 in these strains, whereas a stronger signal for $\alpha 3$ and $\beta 1$ was obtained in P12. In the *P. pastoris* WT + ATPase strain, strongest signals for $\alpha 3$ subunit were seen in P12 and to a lesser extent in P20 and P100. Again, Pma1p was mainly localized in P20. The $\beta 1$ subunit was detected in every pellet together with an additional, smaller band of 35 kDa in fraction P12. This indicates that a certain proportion of $\beta 1$ was not fully glycosylated in this strain.

Remarkably, the expression of $\alpha 3$ and $\beta 1$ in the *P. pastoris* cholesterol strain + ATPase was very strong after 72 h and it also showed co-localization with the plasma membrane in the fractions P20 and P100. The $\beta 1$ subunit was of particular interest, as it is much better expressed than in the control strains. The two bands in the Western blot migrated at apparent sizes of 44 kDa and 40 kDa (see Figure 22), which led to the assumption that $\beta 1$ is glycosylated differently in this strain. Improved expression of $\beta 1$ subunit in the cholesterol-producing *P. pastoris* strain could therefore be the reason for an overall enhanced stability of the heterodimer.

The S100 fraction, referring to the cytosolic compounds, showed no signal for any strain, demonstrating that expression and localization is restricted to membranes.

3.5 Determination of Na,K-ATPase cell surface localization

For this study it was important to know where the heterologously expressed Na,K-ATPase is localized exactly in the cell. Western blot experiments gave first evidence that the ion pump was mainly localized to the plasma membrane. The following section shows the results of further assays that proved that the membrane protein is localized at the surface of the cell.

3.5.1 Cytochrome c reductase assay

Several Western blot experiments were performed using antibodies directed against ER-specific proteins such as Sec61p, Wbp1p or Kar2p. For an unknown reason, the Western blot either gave no signal or the results were not clear. Therefore, a cytochrome c reductase assay was performed to gain an idea about ER localization in the different membrane fractions. Figure 23 shows the results of the assay performed with membrane samples from *P. pastoris* cholesterol strain. It was seen that, corresponding to the protein amount, the

highest activity was found in the P20 fraction. Fractions H, S12, P12, S20 and P100 showed similar reductase activities. As expected, S100, which is mainly the cytosolic fraction, contained only small amounts of cytochrome c reductase. The raw data is given in Table 15.

The assay was performed only with *P. pastoris* WT and cholesterol strain samples, because the distribution is expected to be similar in the other strains.

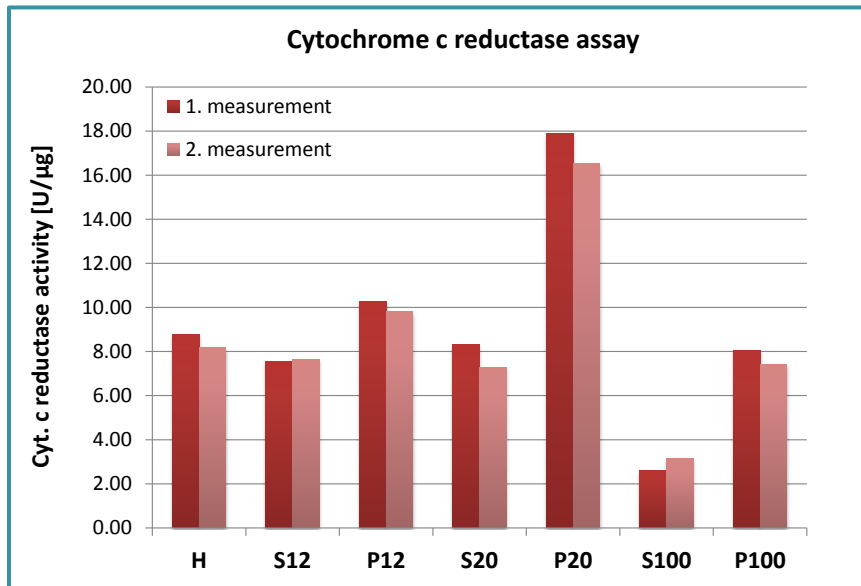


Figure 23. Cytochrome c reductase assay. Samples were taken from *P. pastoris* cholesterol strain membrane preparations after 72 h of induction. **H:** cell homogenate. **S12, P12:** supernatant and pellet at 12,000 x g. **S20, P20:** supernatant and pellet at 20,000 x g. **S100, P100:** supernatant and pellet at 100,000 x g.

TABLE 15. Data obtained from cytochrome c reductase assay with *P. pastoris* cholesterol strain

	H	S12	P12	S20	P20	S100	P100
ΔA550/min	0.0099	0.0077	0.0220	0.0063	0.0182	0.0019	0.0382
	0.0092	0.0078	0.0210	0.0055	0.0168	0.0023	0.0352
U/ml	0.0516	0.0401	0.1147	0.0328	0.0949	0.0099	0.1991
	0.0480	0.0407	0.1095	0.0287	0.0876	0.0120	0.1835
Protein (mg/ml)	5.87	5.31	11.16	3.95	5.3	3.81	24.72
U/μg protein	8.79	7.56	10.28	8.31	17.90	2.60	8.06
	8.17	7.66	9.81	7.26	16.53	3.15	7.42

3.5.2 Na,K-ATPase activity assay

In order to examine the functionality of the heterologously expressed Na,K-ATPase in different strains, release of P_i from ATP hydrolysis was measured. Therefore, a calibration curve was generated using different dilutions of an inorganic phosphate standard (Figure 24). In some experiments, Ca^{2+} or Bafilomycin was added to inhibit the endogenous H^+ -ATPases and reduce the background signal, but the results were not satisfying. Therefore, assays were conducted in presence and absence of ouabain, and the difference was determined as the specific Na,K-ATPase activity. Different membrane fractions were tested after 8 h and 72 h of methanol induction (Figure 25). The values for Na,K-ATPase activities can be seen in detail in Table 16 and Table 17. After 8 h (Figure 25A), measured activity levels were rather low in every strain. Still, slightly increased activity could be seen for the cholesterol-producing strain, especially in the P12 and P100 fractions. The other Na,K-ATPase expressing strains showed similar levels like the negative control strains, indicating that the enzyme was not functional. Striking results can be seen after 72 h of methanol induction (Figure 25B). The *P. pastoris* cholesterol strain clearly surpasses the control strains in every fraction.

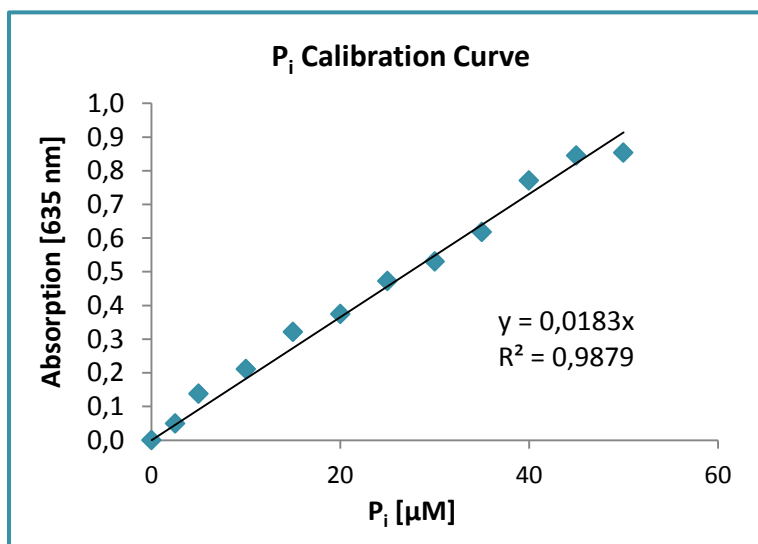


Figure 24. P_i calibration curve. A serial dilution of inorganic phosphate standard was measured photometrically at 635 nm. The equation of the calibration curve was used to determine the amount of hydrolyzed P_i in the samples.

The largest difference can be seen in fractions P20 and P100, which is also consistent with the expression levels detected by Western blot experiments. The *P. pastoris* WT + ATPase, *P. pastoris* SMD1168 + ATPase and *P. pastoris* S- α 3 β 1 + ATPase strains showed activity levels similar to the negative controls.

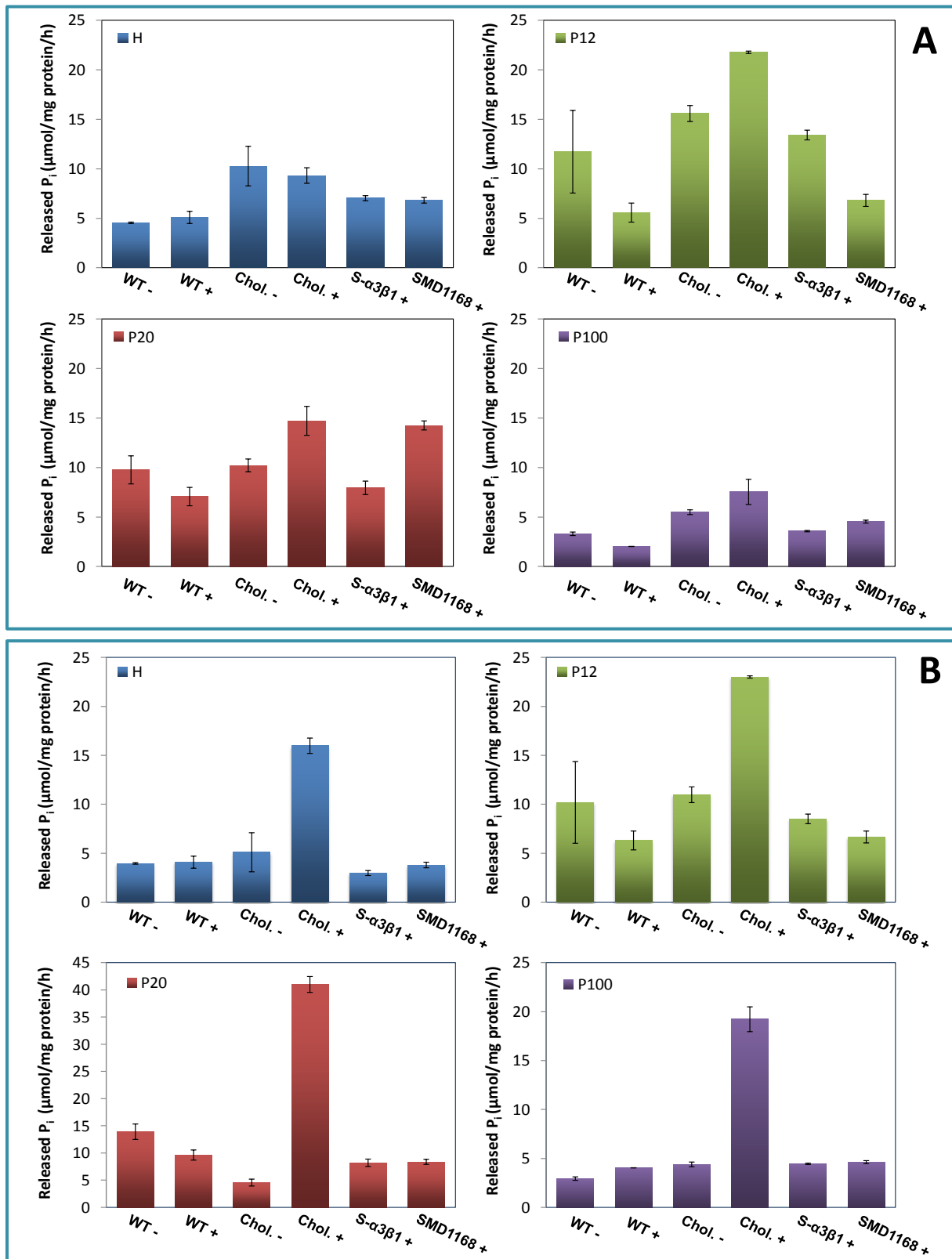


Figure 25. Na,K-ATPase Assay after 8 h and 72 h of methanol induction. Crude membranes were prepared after 8 h (A) and 72 h (B) of induction with methanol. The fractions obtained after centrifugation were: **H** (cell homogenate), **P12** (pellet at 12,000 x g), **P20** (pellet at 20,000 x g) and **P100** (pellet at 100,000 x g). Na,K-ATPase α 3 β 1 isoform expressing strains (+) are compared to the empty *P. pastoris* WT and *P. pastoris* cholesterol-producing strain (-). The bars show the mean value \pm S.E. of measurements in duplicate.

It seems that the specific activity was barely detectable in the crude membrane fractions with this method. Because of the omission of SDS in the assay, a certain part of Na,K-ATPases may be enclosed in sealed right-side-out vesicles and may, therefore, not be accessible by the inhibitor ouabain. Also, the endogenous H⁺-ATPases of yeast may have contributed to the background signals of the empty control strains.

Nevertheless, it was seen clearly that a higher specific Na,K-ATPase activity was measured in the crude membrane fractions of the *P. pastoris* cholesterol-producing strain compared to the other strains. This was achieved without the need of further purification steps or addition of stabilizing agents.

TABLE 16. Na,K-ATPase activities measured after 8 h of induction.

Strain	Released P _i (μmol/mg protein/h)			
	H	P12	P20	P100
<i>P. p.</i> WT	4.54 ± 1.28	11.72 ± 1.43	9.76 ± 2.04	3.30 ± 0.82
<i>P. p.</i> WT + ATPase	5.09 ± 0.17	5.58 ± 2.20	7.06 ± 1.03	2.02 ± 0.07
<i>P. p.</i> Cholesterol strain empty	10.27 ± 0.91	15.59 ± 0.32	10.22 ± 0.18	5.48 ± 2.31
<i>P. p.</i> Cholesterol strain + ATPase	9.32 ± 4.18	21.78 ± 1.97	14.71 ± 1.54	7.53 ± 1.47
<i>P. p.</i> S-α3β1	7.03 ± 0.05	13.41 ± 1.59	7.95 ± 0.62	3.57 ± 0.21
<i>P. p.</i> SMD1168 + ATPase	6.82 ± 0.51	6.81 ± 1.15	14.25 ± 4.47	4.53 ± 0.40

TABLE 17. Na,K-ATPase activities measured after 72 h of induction.

Strain	Released P _i (μmol/mg protein/h)			
	H	P12	P20	P100
<i>P. p.</i> WT	3.96 ± 0.08	10.19 ± 4.17	13.92 ± 1.42	2.94 ± 0.13
<i>P. p.</i> WT + ATPase	4.08 ± 0.61	6.30 ± 0.96	9.62 ± 0.93	4.04 ± 0.01
<i>P. p.</i> Cholesterol strain empty	5.09 ± 2.00	10.97 ± 0.80	4.56 ± 0.64	4.39 ± 0.17
<i>P. p.</i> Cholesterol strain + ATPase	15.98 ± 0.79	23.01 ± 0.12	41.00 ± 1.46	19.22 ± 0.90
<i>P.p.</i> S-α3β1	2.98 ± 0.26	8.51 ± 0.49	8.20 ± 0.68	4.45 ± 0.05
<i>P.p.</i> SMD1168 + ATPase	3.80 ± 0.29	6.65 ± 0.61	8.73 ± 0.46	4.63 ± 0.11

3.5.3 [³H]-Ouabain binding assay

First evidence of plasma membrane localization of the heterologously expressed Na,K-ATPase $\alpha\beta 1$ isoform was given by the Western blot experiments and Na,K-ATPase assays. To prove that a larger amount of Na,K-ATPase is transported and stably inserted into the plasma membrane in the *P. pastoris* cholesterol strain compared to the control strains, the cell surface binding capacity for [³H]-ouabain was investigated. For this purpose, samples were measured by liquid scintillation counting and values for unspecific binding, determined by addition of 1 mM cold ouabain, were subtracted. Raw data is attached in Appendix B. As shown in Figure 26, only small amounts of Na,K-ATPase are present at the surface after 8 h of induction in most of the strains. The *P. pastoris* S- $\alpha\beta 1$ + ATPase strain had even no binding capacity after 8 h. After 72 h, in contrast, binding sites for ouabain were detectable in every strain. The *P. pastoris* SMD1168 + ATPase and *P. pastoris* S- $\alpha\beta 1$ + ATPase strains have a similar binding capacity, which is conclusive as both have the same strain background. However, binding capacity is lower compared to the *P. pastoris* WT + ATPase strain.

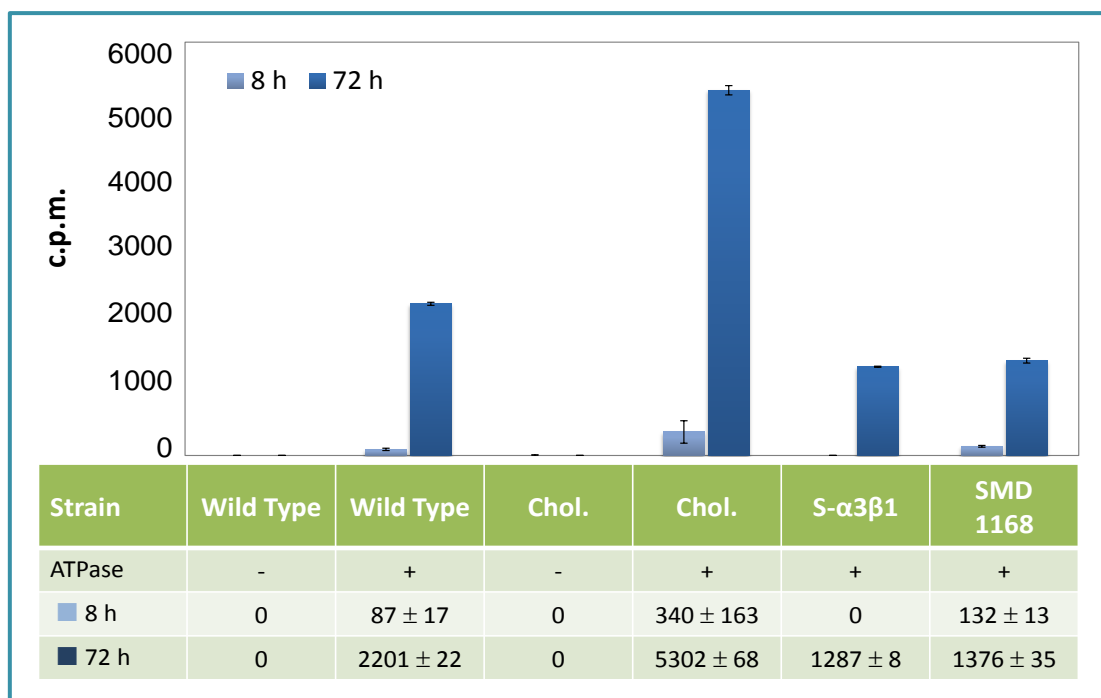


Figure 26. [³H]-ouabain binding assay. Radioligand binding was determined by liquid scintillation counting and values for unspecific binding were subtracted. The bars show the [³H]-ouabain binding capacities for *P. pastoris* WT empty (-), *P. pastoris* WT + ATPase, *P. pastoris* cholesterol strain empty (-), *P. pastoris* cholesterol strain + ATPase, *P. pastoris* S- $\alpha\beta 1$ + ATPase and *P. pastoris* SMD1168 + ATPase. The bars show the mean value ± S.E. of measurements in triplicate.

By plotting the data obtained at different concentrations of [³H]-ouabain in a Scatchard plot (Figure 27), B_{\max} and K_d were calculated. The values are given in Table 18. Remarkably, the *P. pastoris* cholesterol strain had about four times more binding sites at the cell surface (B_{\max}/cell : 478) than the control strains *P. pastoris* SMD1168 + ATPase (B_{\max}/cell : 127) and *P. pastoris* S- $\alpha 3\beta 1$ + ATPase (B_{\max}/cell : 116). The cholesterol strain also had about twice as much binding capacity than the *P. pastoris* WT + ATPase (B_{\max}/cell : 233). The negative controls showed no binding capacity. These data proved that the expression and plasma membrane localization of Na,K-ATPase $\alpha 3\beta 1$ isoform is enhanced in the cholesterol-producing strain.

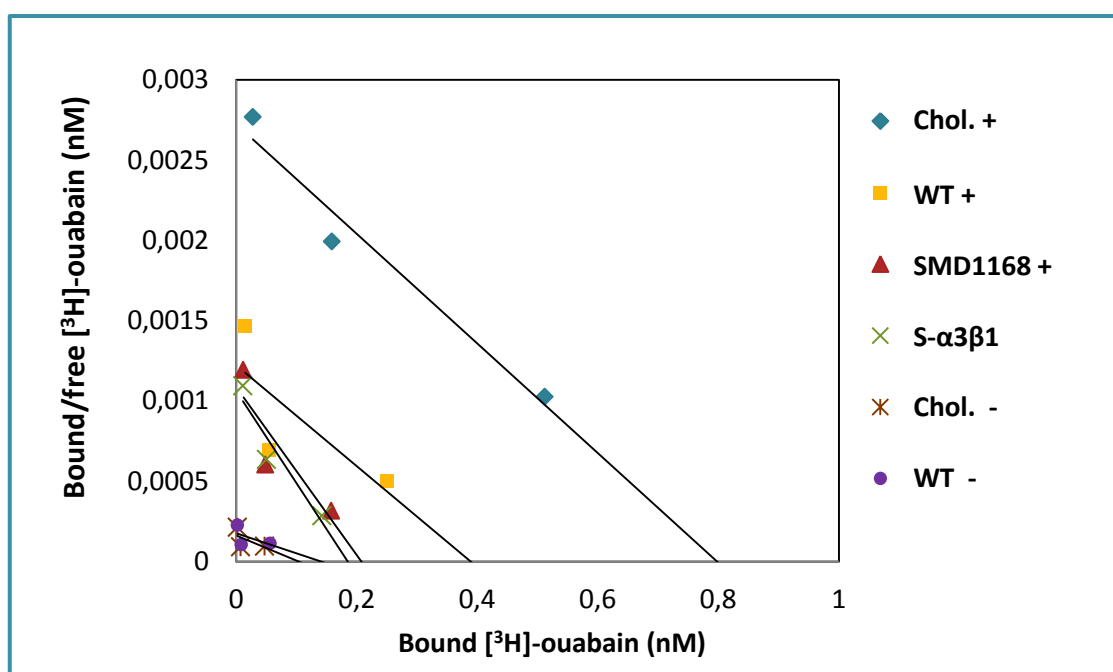


Figure 27. Scatchard plot to determine B_{\max} and K_m of [³H]-ouabain after 72 h of induction. Data was fitted by linear regression to give the cell surface binding capacities (B_{\max}) and dissociation constants (K_d) for ouabain.

TABLE 18. B_{\max}/cell and K_d values for [³ H]-ouabain binding.					
Strain	Linear equation	x-axis intercept	B_{\max}	K_d (nM)	K_d (M)
<i>P. p.</i> WT -	$y = -0.0013x + 0.0002$	0.1538	93	769.23	7.69×10^7
<i>P. p.</i> WT + ATPase	$y = -0.0031x + 0.0012$	0.3871	233	322.58	3.23×10^7
<i>P. p.</i> Chol. -	$y = -0.0016x + 0.0002$	0.1250	75	625.00	6.25×10^7
<i>P. p.</i> Chol. + ATPase	$y = -0.0034x + 0.0027$	0.7941	478	294.12	2.94×10^7
<i>P. p.</i> S- $\alpha 3\beta 1$	$y = -0.0057x + 0.0011$	0.1930	116	175.44	1.75×10^7
<i>P. p.</i> SMD1168 + ATPase	$y = -0.0052x + 0.0011$	0.2115	127	192.31	1.92×10^7

3.5.4 Immunofluorescence

A last experiment was performed by Tamara Wriessnegger to check if the Na,K-ATPase could also be made visible on the cell surface by immunofluorescence microscopy. For these experiments, both available antibodies against $\alpha 3$ or $\beta 1$ subunits were tested. It turned out that better results were achieved with the Anti-KETYY antibody against $\alpha 3$ subunit. The images taken by fluorescence microscopy are shown in Figure 28 and Figure 29. After 8 h of methanol induction, the signal was very low. Nonetheless, spots that might refer to Na,K-ATPase $\alpha 3$ subunit could be detected in the *P. pastoris* SMD1168 + ATPase and S- $\alpha 3\beta 1$ strains. In the cholesterol strain, the whole cells were stained.

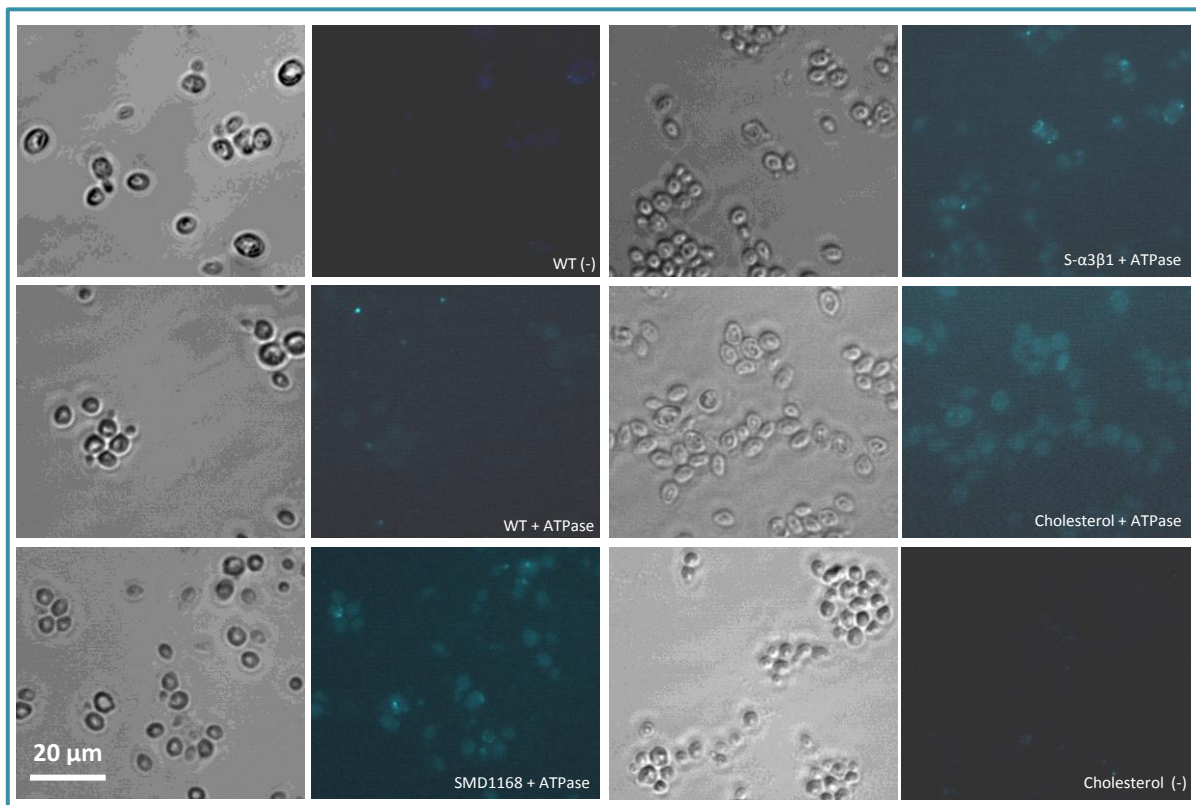


Figure 28. Immunofluorescence microscopy with samples after 8 h of induction. *P. pastoris* cells were incubated with Anti-KETYY antibody against $\alpha 3$ subunit of human Na,K-ATPase.

After 72 h of induction, slight signals could also be detected for the *P. pastoris* WT, and again for *P. pastoris* SMD1168 + ATPase and S- α 3 β 1 strains. The cholesterol strain seemed to have more spots on the surface of the cell, which may refer to the Na,K-ATPase. These results are consistent with those obtained by the [3 H]-ouabain cell surface binding assay. It is consistent that the protease deficient *P. pastoris* SMD1168 and S- α 3 β 1 strains give similar results, whereas the signal for the WT is less than expected. Taken together, the results from the immunofluorescence are not outstanding, but they underline the findings that have been made by the other experiments.

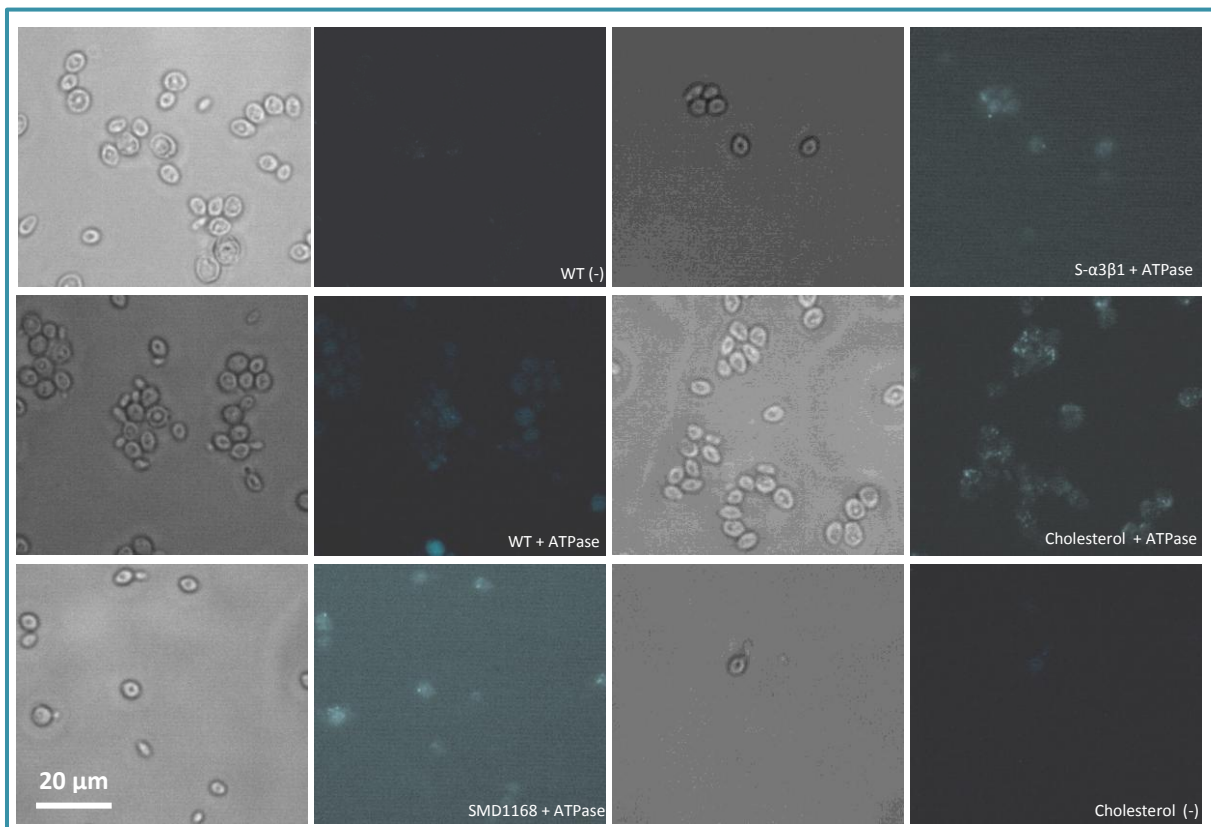


Figure 29. Immunofluorescence microscopy with samples after 72 h of induction. *P. pastoris* cells were incubated with Anti-KETYY antibody against α 3 subunit of human Na,K-ATPase.

4 Discussion

In the present work, the heterologous expression of a human membrane protein, the Na,K-ATPase $\alpha\beta 1$ isoform, was studied in engineered *P. pastoris* strains. It was expected that the different sterols should have a positive effect on the stability and activity of the Na,K-ATPase *in vivo*. Furthermore, the influence of phosphatidylserine should have been tested by generating a *P. pastoris* $\Delta cho1$ knockout strain, which should not be able to produce phosphatidylserine.

The $\Delta cho1$ gene knockout was attempted by integration of a knockout cassette, consisting of 800 bp upstream and downstream homologous regions to the *CHO1* gene and a hygromycin resistance marker (Figure 9). Several clones were tested by colony PCR. On the one hand, the cassette was detectable in the genome of many transformants, but on the other hand all of them still had the *CHO1* gene present (Figure 15). It was assumed that the knockout cassette was indeed incorporated properly, but the replaced DNA sequence had reintegrated somewhere else. To check if the gene was still functional phospholipids were analyzed via thin layer chromatography (Figure 16). The results showed clearly that the knockout had not been successful and all transformants were still capable of producing phosphatidylserine. A new strategy for creating the cassette would be necessary to obtain a proper knockout strain.

Considering that a lack of phosphatidylserine should have a negative influence on the stability of Na,K-ATPase, and the $\Delta cho1$ knockout strain would therefore only be a negative control host, it was decided to focus the work on the existing, membrane engineered strains.

The strains used for the further experiments had been engineered by Tamara Wriessnegger and Gerald Richter in their sterol pathway towards production of alternative sterols, such as campesterol (*P. pastoris* $\Delta erg5::DHCR7$), brassicasterol (*P. pastoris* *DHCR7*) and cholesterol (*P. pastoris* $\Delta erg5::DHCR7\Delta erg6::DHCR24$). These strains were analyzed by GC-MS to examine the sterol pattern. According to GC-MS analyses, about one half of the total sterols in the membrane of *P. pastoris* $\Delta erg5::DHCR7\Delta erg6::DHCR24$ strain were cholesterol. The other half consisted of intermediate products such as cholesta-7,24(25)-dienol, cholesta-5,7,24(25)-trienol and 7-dehydrocholesterol, which are formed during sterol biosynthesis (Figure 4). Although the conversion was not as complete as it was shown for *S. cerevisiae*

with a cholesterol yield of 96% [45], the altered membrane sterol composition still had a notable influence on heterologous expression of human Na,K-ATPase $\alpha 3\beta 1$ isoform.

The growth behavior was examined for all strains used in this work to be able to predict the duration of cultivation experiments. *P. pastoris* $\Delta erg5::DHCR7$, $\Delta erg6::DHCR24$ and cholesterol strains grow slower compared to the *P. pastoris* WT and SMD1168 strains (Figure 13). Apparently, these engineered organisms are restricted in their natural growth behavior due to the production of sterols non-natural for yeast, leading to a diminished specific growth rate. This emphasizes once more the importance of different sterols for the cell physiology of an organism. Despite the delayed growth, cholesterol-producing *P. pastoris* is still capable of reaching high cell densities after longer cultivation times. Also, stable expression of the recombinant Na,K-ATPase $\alpha 3\beta 1$ isoform was facilitated in this strain.

After transformation of different, engineered *P. pastoris* strains, several positive clones were identified by colony PCR and selected for further experiments. A full list of all obtained transformants is given in Table 14. Individual *P. pastoris* transformants were not screened for Mut^S phenotype, because primers for colony PCR were designed in a way to ensure the correct integration into *AOX1* locus. Nonetheless, a strong band for AOX1p at a respective size of 70 kDa could be seen for some strains with Ponceau S staining after blotting. This had, however, no negative influence on protein expression.

To check expression levels of the heterologous protein in selected *P. pastoris* transformants, Western blot experiments were performed on the one hand with the total cell lysate and on the other hand with different membrane fractions. The results showed that the membrane engineered *P. pastoris* *DHCR7*, *P. pastoris* $\Delta erg5::DHCR7$ and *P. pastoris* *cholesterol* strain serve a better environment for stable expression of the $\alpha 3$ subunit, whereas it is less stable and degraded gradually in the *P. pastoris* WT, *P. pastoris* SMD1168 and *P. pastoris* S- $\alpha 3\beta 1$ strains (Figure 20 and Figure 21). Three individual clones of the *P. pastoris* *cholesterol* strain were tested and it turned out that the $\alpha 3$ subunit was well expressed in clone one and two, but the third clone showed bad expression levels. Further work was performed using clone number one.

To reduce the number of samples for membrane preparations, work was limited to six different strains. The most interesting and important *P. pastoris* *cholesterol* + ATPase strain

was cultivated together with *P. pastoris* WT and SMD1168 strains expressing the Na,K-ATPase. To be able to compare the experiments with already published data, the *P. pastoris* S- $\alpha 3\beta 1$ strain, which also has the SMD1168 background, was examined. *P. pastoris* WT and *P. pastoris* cholesterol strain without the expression plasmid served as negative controls.

Western blot experiments from membrane preparations revealed that especially the $\beta 1$ subunit is much better expressed in the *P. pastoris* cholesterol strain. In this strain, both subunits were detected in the same fractions as plasma membrane marker Pma1p, suggesting the co-localization of the protein with the plasma membrane (Figure 22).

Earlier, it had been demonstrated that expression of the α subunit without the β subunit leads to ER retention and degradation [22,36,55]. This correlates with observations made in this work. In strains which are badly expressing the $\beta 1$ subunit also $\alpha 3$ subunit is susceptible to degradation. In the cholesterol strain, in contrast, the $\beta 1$ subunit was very well expressed and, therefore, stabilized the $\alpha 3$ subunit promoting transport and correct integration into the plasma membrane. Cholesterol was recently found to be associated with Tyr⁴⁰ of the β subunit in the crystal structure of Na,K-ATPase [29]. This amino acid forms a hydrogen bond with Gln⁸⁵⁶ on transmembrane domain 7 of the α subunit. This highly conserved tyrosine residue was also previously described to interact with the α subunit [56]. Consequently, the cholesterol in the membranes of the engineered *P. pastoris* strain interacts with the $\beta 1$ subunit, hence improving the assembly of the recombinant $\alpha 3$ - $\beta 1$ dimer. This could explain overall, why the cholesterol strain provides a better environment to form a functional and stable recombinant Na,K-ATPase.

The β subunit is a 35 kDa protein with three glycosylation sites [57], which leads to an apparent size of 55 kDa in mammalian cells, but only 44 kDa in *P. pastoris* due to different glycosylation patterns. Observations in this work showed that in the *P. pastoris* cholesterol + ATPase strain an additional 40 kDa protein is produced. In the WT + ATPase strain, in contrast, a protein with an apparent size of 35 kDa can be detected besides the 44 kDa band. Similar findings have also been described earlier [22,38]. This leads to the assumption that glycosylation is performed differently in the *P. pastoris* cholesterol strain, probably also contributing to the subunit assembly. It is described though, that only the complete lack of glycosylated β subunits influences the assembly and activity of Na,K-ATPase negatively [58].

Na,K-ATPase assays proved that the enzyme was active in different membrane fractions of the *P. pastoris* cholesterol + ATPase strain. It was possible to specifically detect Na,K-ATPase activity in crude membrane fractions without further purification steps or the addition of stabilizing lipids as they were described for example in Refs. [11] and [28]. In accordance with the Western blot results, the highest activity was measured in the P20 fraction ($41.00 \pm 1.46 \mu\text{mol P}_i/\text{mg protein/h}$). Also, the measured activity relative to the control strains in the P100 fraction ($19.22 \pm 0.9 \mu\text{mol P}_i/\text{mg protein/h}$) is outstanding for the cholesterol-producing yeast. Already published data gave the information that the α - β complex is assembled in the ER where the protein already performs its function [36]. This could be a possible reason for the detection of specific Na,K-ATPase activity in fractions containing membrane parts other than the plasma membrane. Cytochrome c reductase assays revealed that the ER is also distributed over the fractions, peaking in fraction P20 (Figure 23). This showed that the subfractions of plasma membrane and ER were not clearly distinguishable. Performing membrane fractionation with density gradient centrifugation would have presumably worked better for this purpose.

Surprisingly, the *P. pastoris* WT + ATPase, SMD1168 + ATPase and S- α 3 β 1 + ATPase strains gave signals for Na,K-ATPase activity similar to the control strains not expressing Na,K-ATPase. As discussed earlier, this may be due to inferior expression of the β 1 subunit, which leads to impaired stability of the protein in the ergosterol-containing membranes resulting in diminished activity of the expression strains. Furthermore, SDS is routinely used for purification, solubilization and demasking of Na,K-ATPases that are enclosed in sealed vesicles and, therefore, accessibility by either ouabain or ATP is reduced [59]. Preceding incubation of membranes with SDS had been shown to inhibit yeast endogenous H^+ -ATPases and, furthermore, had increased Na,K-ATPase activity by 20 % due to improved accessibility of Na,K-ATPases in closed vesicles [19]. To preserve the natural membrane environment, the assay setup did not include SDS treatment of the membranes and, therefore, this had to be taken into account. The measured ATP hydrolysis of the non-expressing strains could therefore refer to background signals. Nonetheless, focus should be brought into the measured Na,K-ATPase activity in the membrane fractions of the *P. pastoris* cholesterol strain, as it clearly surpasses the activities of all other control strains in this study.

Investigation of expression levels by Western blot analyses and Na,K-ATPase activities gave first evidence for recombinant protein localization in the plasma membrane. Additionally, it was of great interest how much of the protein is effectively transported to the surface of the cell. This was done by radioligand binding studies of [³H]-ouabain to intact cells. The inhibitor binds specifically to the Na,K-ATPase α -subunit at the outside of intact cells and can, therefore, be used to trace the sodium pump in the yeast plasma membrane. The cell surface [³H]-ouabain binding capacity for the *P. pastoris* S- α 3 β 1 strain, which was used for control experiments, correlated well with already published data [22]. Strikingly, the cholesterol strain showed about four times more surface binding sites for ouabain, proving that the Na,K-ATPase is located on the cell surface to a higher extent compared to the control strains. The B_{\max} values obtained for the empty control strains refer to unspecific binding of [³H]-ouabain to the cell surface and can be neglected.

Immunofluorescence microscopy was carried out by Tamara Wriessnegger to make the Na,K-ATPase visible at the cell surface (Figure 28, Figure 29). Incubation with Anti-KETYY antibody against the α subunit gave signals for the cholesterol strain especially after 72 h of induction. Fluorescence signals could also be detected for *P. pastoris* SMD1168 and S- α 3 β 1 strains, although it was difficult to quantify signal strength. Nevertheless, the microscopic images were consistent with Na,K-ATPase α 3 β 1 expressed on the cell surface.

Low Na,K-ATPase activities and inefficient transport to the plasma membrane as described by Reina et al. [22] were therefore significantly enhanced by using a cholesterol-producing *P. pastoris* strain as expression host. The improvement can be directly seen in comparison with the *P. pastoris* S- α 3 β 1 strain.

It has been shown that expression of the Na,K-ATPase α 3 β 1 is limited in shaking flask cultures, but could be improved by cultivating cells in a fermenter [22]. As all studies were performed in shaking flasks and the results showed that the expression was improved in the cholesterol strain, these positive effects may become even more evident by optimizing the cultivation parameters.

Although attempts have been made earlier to create a *S. cerevisiae* cholesterol strain for enhanced membrane protein production [60], this work provides the first evidence that

expression of a human membrane protein is improved in a yeast strain capable of producing cholesterol instead of ergosterol.

To conclude, the results of this work clearly show that changing the lipid environment of a heterologous host system such as *P. pastoris* largely contributes to the improvement of recombinant expression and stability of a human membrane protein known for its interaction with cholesterol.

5 Outlook

This work provides first biochemical analyses on the already well-characterized human Na,K-ATPase expressed in different membrane engineered *P. pastoris* strains. Unfortunately, not all of the interesting engineered strains could be characterized in detail. A lot of potential might also lie in these strains, as the first Western blot experiments clearly showed. Especially *P. pastoris* $\Delta erg5::DHCR7$ and *P. pastoris* *DHCR7* strains lacking the 5, 7 conjugated double bond seemed auspicious. Nevertheless, focus was brought to the cholesterol-producing strain, which gave very promising results for the expression of Na,K-ATPase $\alpha 3\beta 1$ isoform. For future work, it would be interesting to examine the stability and activity of other recombinant Na,K-ATPase isoforms as well. Moreover, cholesterol producing yeasts might allow production of higher amounts of functional and stable mammalian membrane proteins, which are useful for biochemical and structural studies as well as drug development processes.

6 References

1. Freigassner, M., Pichler, H. and Glieder, A. (2009) Tuning microbial hosts for membrane protein production. *Microbial Cell Factories* **8**, 69.
2. Opekarová, M. and Tanner, W. (2003) Specific lipid requirements of membrane proteins - a putative bottleneck in heterologous expression. *Biochim Biophys Acta* **1610**, 11-22.
3. Skou, J. C. (1957) The influence of some cations on an adenosine triphosphatase from peripheral nerves. *Biochim Biophys Acta* **23**, 394-401.
4. Kaplan, J. H. (2002) Biochemistry of Na,K-ATPase. *Annu Rev Biochem* **71**, 511-535.
5. Geering, K. (2006) FXYD proteins: new regulators of Na-K-ATPase. *Am J Physiol Renal Physiol* **290**, F241-F250.
6. Aperia, A. (2007) New roles for an old enzyme: Na,K-ATPase emerges as an interesting drug target. *Journal of Internal Medicine* **261**, 44-52.
7. Schwinger, R. H. G., Bundgaard, H., Müller-Ehmsen, J. and Kjeldsen, K. (2003) The Na,K-ATPase in the failing human heart. *Cardiovascular Research* **57**, 913-920.
8. Sweadner, K. J. (1990) Anomalies in the electrophoretic resolution of Na⁺/K⁺-ATPase catalytic subunit isoforms reveal unusual protein-detergent interactions. *Biochim Biophys Acta* **1029**, 13-23.
9. Bøttger, P., Tracz, Z., Heuck, A., Nissen, P., Romero-Ramos, M. and Lykke-Hartmann, K. (2011) Distribution of Na/K-ATPase alpha 3 isoform, a sodium-potassium P-type pump associated with rapid-onset of dystonia parkinsonism (RDP) in the adult mouse brain. *J Comp Neurol* **519**, 376-404.
10. Blanco, G. and Mercer, R. W. (1998) Isozymes of the Na-K-ATPase: heterogeneity in structure, diversity in function. *Am J Physiol Renal Physiol* **275**, F633-F650.
11. Lifshitz, Y., Petrovich, E., Haviv, H., Goldshleger, R., Tal, D. M., Garty, H. and Karlish, S. J. D. (2007) Purification of the human alpha2 Isoform of Na,K-ATPase expressed in *Pichia pastoris*. Stabilization by lipids and FXYD1. *Biochemistry* **46**, 14937-14950.
12. Cirri, E., Katz, A., Mishra, N. K., Belogus, T., Lifshitz, Y., Garty, H., Karlish, S. J. D. and Apell, H.-J. (2011) Phospholemmann (FXYD1) raises the affinity of the human $\alpha 1\beta 1$ isoform of Na,K-ATPase for Na ions. *Biochemistry* **50**, 3736-3748.
13. Mishra, N. K., Peleg, Y., Cirri, E., Belogus, T., Lifshitz, Y., Voelker, D. R., Apell, H.-J., Garty, H. and Karlish, S. J. D. (2011) FXYD proteins stabilize Na,K-ATPase: amplification of specific phosphatidylserine-protein interactions. *J Biol Chem* **286**, 9699-9712.

14. Geering, K. (2001) The functional role of beta subunits in oligomeric P-type ATPases. *J Bioenerg Biomembr* **33**, 425-438.
15. Hasler, U., Wang, X., Crambert, G., Béguin, P., Jaisser, F., Horisberger, J.-D. and Geering, K. (1998) Role of Beta-Subunit Domains in the Assembly, Stable Expression, Intracellular Routing, and Functional Properties of Na,K-ATPase. *J Biol Chem* **273**, 30826-30835.
16. Béguin, P., Hasler, U., Beggah, A., Horisberger, J. D. and Geering, K. (1998) Membrane integration of Na,K-ATPase alpha-subunits and beta-subunit assembly. *J Biol Chem* **273**, 24921-24931.
17. Crambert, G., Hasler, U., Beggah, A. T., Yu, C., Modyanov, N. N., Horisberger, J.-daniel, Lelièvre, L. and Geering, K. (2000) Transport and Pharmacological Properties of Nine Different Human Na,K-ATPase Isozymes. *J Biol Chem* **275**, 1976 -1986.
18. Müller-Ehmsen, J., Juvvadi, P., Thompson, C. B., Tumyan, L., Croyle, M., Lingrel, J. B., Schwinger, R. H. G., McDonough, A. A. and Farley, R. A. (2001) Ouabain and substrate affinities of human Na⁺,K⁺-ATPase $\alpha 1\beta 1$, $\alpha 2\beta 1$, and $\alpha 3\beta 1$ when expressed separately in yeast cells. *American Journal of Physiology. Cell physiology* **281**, C1355-C1364.
19. Pedersen, P. A., Rasmussen, J. H. and Jørgensen, P. L. (1996) Expression in high yield of pig alpha1 beta1 Na,K-ATPase and inactive mutants D369N and D807N in *Saccharomyces cerevisiae*. *J Biol Chem* **271**, 2514-2522.
20. Horowitz, B., Eakle, K. A., Scheiner-Bobis, G., Randolph, G. R., Chen, C. Y., Hitzeman, R. A. and Farley, R. A. (1990) Synthesis and Assembly of Functional Mammalian Na,K-ATPase in Yeast. *J Biol Chem* **265**, 4189-4192.
21. Cohen, E., Goldshleger, R., Shainskaya, A., Tal, D. M., Ebel, C., Le Maire, M. and Karlish, S. J. D. (2005) Purification of Na⁺,K⁺-ATPase expressed in *Pichia pastoris* reveals an essential role of phospholipid-protein interactions. *J Biol Chem* **280**, 16610-16618.
22. Reina, C., Padoani, G., Carotti, C., Merico, A., Tripodi, G., Ferrari, P. and Popolo, L. (2007) Expression of the alpha3/beta1 isoform of human Na,K-ATPase in the methylotrophic yeast *Pichia pastoris*. *FEMS Yeast Res* **7**, 585-594.
23. Blanco, G. (2005) The NA/K-ATPase and its isozymes: what we have learned using the baculovirus expression system. *Front Biosci* **10**, 2397-2411.
24. Liu, J. Y. and Guidotti, G. (1997) Biochemical characterization of the subunits of the Na⁺/K⁺ ATPase expressed in insect cells. *Biochim Biophys Acta* **1336**, 370-386.
25. Koenderink, J. B., Swarts, H. G., Hermsen, H. P., Willems, P. H. and De Pont, J. J. (2000) Mutation of aspartate 804 of Na(+),K(+)-ATPase modifies the cation binding pocket and thereby generates a high Na(+)-ATPase activity. *Biochemistry* **39**, 9959-9966.

26. Cornelius, F. (2001) Modulation of Na⁺, K-ATPase and Na-ATPase Activity by Phospholipids and Cholesterol. I. Steady-State Kinetics. *Biochemistry* **40**, 8842-8851.
27. Cornelius, F., Turner, N. and Christensen, H. R. Z. (2003) Modulation of Na,K-ATPase by Phospholipids and Cholesterol. II. Steady-State and Presteady-State Kinetics. *Biochemistry* **42**, 8541-8549.
28. Haviv, H., Cohen, E., Lifshitz, Y., Tal, D. M., Goldshleger, R. and Karlsh, S. J. D. (2007) Stabilization of Na⁺,K⁺-ATPase purified from *Pichia pastoris* membranes by specific interactions with lipids. *Biochemistry* **46**, 12855-12867.
29. Toyoshima, C., Kanai, R. and Cornelius, F. (2011) First crystal structures of Na⁺,K⁺-ATPase: new light on the oldest ion pump. *Structure* **19**, 1732-1738.
30. Adamian, L., Naveed, H. and Liang, J. (2011) Lipid-binding surfaces of membrane proteins: evidence from evolutionary and structural analysis. *Biochim Biophys Acta* **1808**, 1092-1102.
31. Hanson, M. A., Cherezov, V., Griffith, M. T., Roth, C. B., Jaakola, V.-P., Chien, E. Y. T., Velasquez, J., Kuhn, P. and Stevens, R. C. (2008) A specific cholesterol binding site is established by the 2.8 Å structure of the human beta2-adrenergic receptor. *Structure* **16**, 897-905.
32. Burger, K., Gimpl, G. and Fahrenholz, F. (2000) Regulation of receptor function by cholesterol. *Cell Mol Life Sci* **57**, 1577-1592.
33. Xu, X., Bittman, R., Duportail, G., Heissler, D., Vilcheze, C. and London, E. (2001) Effect of the structure of natural sterols and sphingolipids on the formation of ordered sphingolipid/sterol domains (rafts). Comparison of cholesterol to plant, fungal, and disease-associated sterols and comparison of sphingomyelin, cerebroside, and ceramide. *J Biol Chem* **276**, 33540-33546.
34. Nes, W. D. (2011) Biosynthesis of cholesterol and other sterols. *Chem Rev* **111**, 6423-6451.
35. Bill, R. M. (2001) Yeast - a panacea for the structure-function analysis of membrane proteins? *Curr Genet* **40**, 157-171.
36. Gatto, C., McCloud, S. M. and Kaplan, J. H. (2001) Heterologous expression of Na⁺-K⁺-ATPase in insect cells: intracellular distribution of pump subunits. *American Journal of Physiology. Cell Physiology* **281**, C982-C992.
37. Ramón, A. and Marín, M. (2011) Advances in the production of membrane proteins in *Pichia pastoris*. *Biotechnology Journal* **6**, 700-706.
38. Katz, A., Lifshitz, Y., Bab-Dinitz, E., Kapri-Pardes, E., Goldshleger, R., Tal, D. M. and Karlsh, S. J. D. (2010) Selectivity of digitalis glycosides for isoforms of human Na,K-ATPase. *J Biol Chem* **285**, 19582-19592.

39. Strugatsky, D., Gottschalk, K.-E., Goldshleger, R., Bibi, E. and Karlish, S. J. D. (2003) Expression of Na⁺,K⁺-ATPase in *Pichia pastoris*: analysis of wild type and D369N mutant proteins by Fe²⁺-catalyzed oxidative cleavage and molecular modeling. *J Biol Chem* **278**, 46064-46073.
40. Zeder-Lutz, G., Cherouati, N., Reinhart, C., Pattus, F. and Wagner, R. (2006) Dot-blot immunodetection as a versatile and high-throughput assay to evaluate recombinant GPCRs produced in the yeast *Pichia pastoris*. *Protein Expression and Purification* **50**, 118-127.
41. Mao, Q., Gwenaelle, C., Gupta, A., Cole, S. P. C. and Unadkat, J. D. (2004) Functional expression of the human breast cancer resistance protein in *Pichia pastoris*. *Biochemical and Biophysical Research Communications* **320**, 730-737.
42. Chloupková, M., Pickert, A., Lee, J.-Y., Souza, S., Trinh, Y. T., Connelly, S. M., Dumont, M. E., Dean, M. and Urbatsch, I. L. (2007) Expression of 25 human ABC transporters in the yeast *Pichia pastoris* and characterization of the purified ABCC3 ATPase activity. *Biochemistry* **46**, 7992-8003.
43. Asada, H., Uemura, T., Yurugi-Kobayashi, T., Shiroishi, M., Shimamura, T., Tsujimoto, H., Ito, K., Sugawara, T., Nakane, T., Nomura, N., et al. (2011) Evaluation of the *Pichia pastoris* expression system for the production of GPCRs for structural analysis. *Microb Cell Fact* **10**, 24.
44. Richter, G. (2011) Membrane Engineering in Yeast. Master's thesis, Graz University of Technology, Austria.
45. Souza, C. M., Schwabe, T. M. E., Pichler, H., Ploier, B., Leitner, E., Guan, X. L., Wenk, M. R., Riezman, I. and Riezman, H. (2011) A stable yeast strain efficiently producing cholesterol instead of ergosterol is functional for tryptophan uptake, but not weak organic acid resistance. *Metab Eng* **13**, 555-569.
46. Näätsaari, L., Mistlberger, B., Ruth, C., Hajek, T., Hartner, F. S. and Glieder, A. (2012) Deletion of the *Pichia pastoris* KU70 Homologue Facilitates Platform Strain Generation for Gene Expression and Synthetic Biology. *PLoS One* **7**, e39720.
47. Schneiter, R. and Daum, G. (2006) Extraction of Yeast Lipids. *Yeast Protocols: Methods in Molecular Biology* **313**, 41-45.
48. Vaden, D. L., Gohil, V. M., Gu, Z. and Greenberg, M. L. (2005) Separation of yeast phospholipids using one-dimensional thin-layer chromatography. *Analytical Biochemistry* **338**, 162-164.
49. Alberts, B., Johnson, A., Lewis, J., Raff, M., Keith, R. and Walter, P. (2002) *Molecular Biology of the Cell* 4th edition, p. 479, Garland Science, New York.
50. Lowry, O. H., Rosebrough, N. J., Farr, L. A. and Randall, R. J. (1951) Protein Measurement with the Folin Phenol Reagent. *J Biol Chem* **193**, 265-276.

51. Kapri-Pardes, E., Katz, A., Haviv, H., Mahmoud, Y., Ilan, M., Khalfin-Penigel, I., Carmeli, S., Yarden, O. and Karlisch, S. J. D. (2011) Stabilization of the alpha2 Isoform of Na,K-ATPase by Mutations in a Phospholipid Binding Pocket. *J Biol Chem* **286**, 42888 - 42899.
52. Gordon, J. A. (1991) Use of vanadate as protein-phosphotyrosine phosphatase inhibitor. *Methods Enzymol* **201**, 477-82.
53. Pedersen, P. A., Rasmussen, J. H. and Jørgensen, P. L. (1996) Consequences of mutations to the phosphorylation site of the alpha-subunit of Na, K-ATPase for ATP binding and E1-E2 conformational equilibrium. *Biochemistry* **35**, 16085-16093.
54. Scatchard, G. (1949) The attractions of proteins for small molecules and ions. *Ann N Y Acad Sci* **51**, 660-672.
55. Beggah, A., Mathews, P., Beguin, P. and Geering, K. (1996) Degradation and endoplasmic reticulum retention of unassembled alpha- and beta-subunits of Na,K-ATPase correlate with interaction of BiP. *J Biol Chem* **271**, 20895-20902.
56. Hasler, U., Crambert, G., Horisberger, J. D. and Geering, K. (2001) Structural and functional features of the transmembrane domain of the Na,K-ATPase beta subunit revealed by tryptophan scanning. *J Biol Chem* **276**, 16356-16364.
57. Ovchinnikov Y. A., Modyanov, N. N., Broude, N. E., Petrukhin, K. E., Grishin, A. V., Arzamazova, N. M., Aldanova, N. A., Monastyrskaya, G. S. and Sverdlov, E. D. (1986) Pig kidney Na⁺,K⁺-ATPase. Primary structure and spatial organization. *FEBS Lett* **201**, 237-245.
58. Beggah, A. T., Jaunin, P. and Geering, K. (1997) Role of glycosylation and disulfide bond formation in the beta subunit in the folding and functional expression of Na,K-ATPase. *J Biol Chem* **272**, 10318-10326.
59. Ivanov, A. V., Gable, M. E. and Askari, A. (2004) Interaction of SDS with Na⁺/K⁺-ATPase: SDS-solubilized enzyme retains partial structure and function. *J Biol Chem* **279**, 29832-29840.
60. Kitson, S. M., Mullen, W., Cogdell, R. J., Bill, R. M. and Fraser, N. J. (2011) GPCR production in a novel yeast strain that makes cholesterol-like sterols. *Methods, Elsevier Inc.* **55**, 287-292.

7 List of figures

FIGURE NO.	PAGE
Figure 1. 2.80 Å crystal structure of Na,K-ATPase with ligands	10
Figure 2. Structures of ergosterol and cholesterol	11
Figure 3. Microscopic image of <i>P. pastoris</i> cells,	12
Figure 4. Sterol pattern of <i>P. pastoris</i> WT and <i>P. pastoris</i> cholesterol-producing strain	13
Figure 5. Expression vector pAO815- $\alpha 3\beta 1$	21
Figure 6. Expression vector pAG32-HPH	22
Figure 7. pJET1.2/blunt- $\Delta cho1$ vector	22
Figure 8. GeneRuler™ 1 kb Plus DNA Ladder and GeneRuler™ DNA Ladder Mix.....	26
Figure 9. Phosphatidyl serine synthase (<i>CHO1</i>) knockout cassette	28
Figure 10. Differential centrifugation	35
Figure 11. Neubauer improved counting chamber	41
Figure 12. Liquid Scintillation Analyzer Tri-Carb2900TR	45
Figure 13. <i>P. pastoris</i> growth curves on BMGY media	47
Figure 14. Construction of <i>CHO1</i> knockout cassette via overlap extension PCR	48
Figure 15. Colony PCR of different <i>P. pastoris</i> $\Delta cho1$ knockout mutants	49
Figure 16. Thin-layer chromatography for analysis of <i>P. pastoris</i> phospholipids	50
Figure 17. Plasmid pAO815 $\alpha 3\beta 1$ after linearization with <i>Bgl</i> II.....	51
Figure 18. Colony PCR of selected clones after transformation with pAO815- $\alpha 3\beta 1$ vector. ...	52
Figure 19. Calibration curve for protein quantification using the Lowry-method.....	53
Figure 20. Western blot experiments	54
Figure 21. Western blot experiments of Na,K-ATPase expressing strains	55
Figure 22. Western blot experiments with membrane fractions	57
Figure 23. Cytochrome c reductase assay	59
Figure 24. P_i calibration curve	60
Figure 25. Na,K-ATPase Assay after 8 h and 72 h of methanol induction	61
Figure 26. [3 H]-ouabain binding Assay	63
Figure 27. Scatchard plot to determine B_{max} and K_m of [3 H]-ouabain	64
Figure 28. Immunofluorescence microscopy with samples after 8 h of induction	65
Figure 29. Immunofluorescence microscopy with samples after 24 h of induction	66

8 List of tables

TABLE NO.	PAGE
TABLE 1. Suppliers of reagents used in this study.....	14
TABLE 2. Solutions and Media used	16
TABLE 3. Instruments and Devices used in this work.....	19
TABLE 4. <i>P. pastoris</i> and <i>E. coli</i> strain used in this study	20
TABLE 5. Primers for cPCR verification of <i>P. pastoris</i> transformants.....	23
TABLE 6. Primers for construction of <i>CHO1</i> knockout cassette	23
TABLE 7. Primers for cPCR verification of <i>P. pastoris</i> $\Delta cho1$ knockout mutants	24
TABLE 8. Primers for Sequencing of <i>P. pastoris</i> $\Delta cho1$ knockout mutants	24
TABLE 9. Adjustments for GC-MS analysis of total sterols from <i>P. pastoris</i>	32
TABLE 10. Composition of self made SDS-PAGE gels.	37
TABLE 11. Cell counting after 8 h of methanol induction	42
TABLE 12. Cell counting after 24 h of methanol induction	42
TABLE 13. Specific growth rates of different <i>P. pastoris</i> strains.....	47
TABLE 14. Positive <i>P. pastoris</i> transformants containing Na,K-ATPase expression cassette	52
TABLE 15. Data obtained from cytochrome c reductase assay	59
TABLE 16. Na,K-ATPase activities measured after 8 h of induction.....	62
TABLE 17. Na,K-ATPase activities measured after 72 h of induction.....	62
TABLE 18. $B_{max}/cell$ and K_d values for [3H]-ouabain binding.	64

9 Appendices

Appendix A: Protein determination

APPENDIX A TABLE 1. Protein concentration of small scale cultivation samples.					
Sample	Protein [mg/ml]	Sample	Protein [mg/ml]	Sample	Protein [mg/ml]
WT t0 (-)	1.61	SMD1168 1 t0	1.07	erg5 1 t0	1.11
WT t8 (-)	1.47	SMD1168 1 t8	2.00	erg5 1 t8	2.59
WT t24 (-)	1.23	SMD1168 1 t24	2.45	erg5 1 t24	2.87
WT t48 (-)	1.14	SMD1168 1 t48	2.57	erg5 1 t48	2.41
WT t72 (+)	1.81	SMD1168 1 t72	2.40	erg5 1 t72	2.52
S- α 3 β 1 t0 (-)	0.80	SMD1168 2 t0	1.66	erg5 2 t0	1.31
S- α 3 β 1 t8 (-)	1.55	SMD1168 2 t8	2.49	erg5 2 t8	1.46
S- α 3 β 1 t24 (-)	2.72	SMD1168 2 t24	3.06	erg5 2 t24	3.20
S- α 3 β 1 t48 (-)	2.13	SMD1168 2 t48	3.44	erg5 2 t48	2.55
S- α 3 β 1 t72 (-)	4.15	SMD1168 2 t72	2.50	erg5 2 t72	3.27
WT 1 t0	1.44	DHCR7 1 t0	3.20	erg5 3 t0	1.35
WT 1 t8	2.87	DHCR7 1 t8	3.09	erg5 3 t8	2.37
WT 1 t24	2.65	DHCR7 1 t24	5.80	erg5 3 t24	2.95
WT 1 t48	3.20	DHCR7 1 t48	5.35	erg5 3 t48	2.74
WT 1 t72	2.54	DHCR7 1 t72	4.48	erg5 3 t72	3.01
WT 2 t0	2.17	DHCR7 2 t0	2.05	Cholesterol 3 t0	1.13
WT 2 t8	2.22	DHCR7 2 t8	1.85	Cholesterol 3 t8	1.73
WT 2 t24	3.10	DHCR7 2 t24	5.30	Cholesterol 3 t24	1.18
WT 2 t48	3.11	DHCR7 2 t48	4.80	Cholesterol 3 t48	1.12
WT 2 t72	3.02	DHCR7 2 t72	4.15	Cholesterol 3 t72	1.14
Cholesterol 1 t0	0.72	Cholesterol 2 t0	0.96		
Cholesterol 1 t8	0.70	Cholesterol 2 t8	1.03		
Cholesterol 1 t24	1.12	Cholesterol 2 t24	1.08		
Cholesterol 1 t48	0.94	Cholesterol 2 t48	0.97		
Cholesterol 1 t72	1.10	Cholesterol 2 t72	1.37		

APPENDIX A TABLE 2. Protein concentration of large scale cultivation samples after 8 h of induction.

Protein amount (mg/ml)							
	H	S12	P12	S20	P20	S100	P100
WT	11.85	9.17	22.52	8.74	10.61	5.80	21.67
WT + ATPase	17.31	14.40	27.88	13.68	13.58	5.26	32.64
Cholesterol	6.43	4.95	10.95	5.56	5.45	2.07	20.53
Chol. + ATPase	5.01	4.34	7.26	4.26	4.39	1.89	16.75
S- α 3 β 1	10.47	8.37	16.57	7.70	7.14	2.72	20.36
SMD1168 + ATPase	11.20	7.88	20.23	6.21	7.83	4.07	25.78

APPENDIX A TABLE 3. Protein concentration of large scale cultivation samples after 72 h of induction.

Protein amount (mg/ml)							
	H	S12	P12	S20	P20	S100	P100
WT	9.69	6.03	12.46	5.60	11.93	3.98	28.13
WT + ATPase	23.05	19.21	34.30	16.00	15.13	4.98	29.63
Cholesterol	8.78	7.57	15.06	5.14	12.24	2.88	25.69
Chol. + ATPase	5.87	5.31	11.16	3.95	5.30	3.81	24.72
S- α 3 β 1	15.55	12.42	28.44	12.61	9.86	4.83	28.70
SMD1168 + ATPase	8.00	6.54	19.38	4.78	5.84	3.33	16.53

Appendix B: [³H]-ouabain binding data

APPENDIX B TABLE 1. Data evaluation for the Scatchard plot.

Strain	c.p.m.	c.p.m./20 μ l	Free ligand	Ratio bound/ free ligand	Bound Ouabain (nM)	Linear Equation	x-axis intercept	B _{max}	K _d (nM)	K _d (M)
<i>P. p.</i> WT -	700	6242524	500 nM	6241824	0.0001122	0.056093764				
	114	1091464	80 nM	1091350	0.000104152	0.008331318	$y = -0.0013x + 0.0002$	0.1538	93	769.23
	26	113268	10 nM	113242	0.000226653	0.002266012				
<i>P. p.</i> WT + ATPase	3116	6242524	500 nM	6239408	0.000499406	0.249578536				
	757	1091464	80 nM	1090707	0.000694351	0.055509542	$y = -0.0031x + 0.0012$	0.3871	233	322.58
	166	113268	10 nM	113102	0.001467702	0.014655507				
<i>P. p.</i> Chol. -	593	6242524	500 nM	6241931	9.49492E-05	0.047470115				
	100	1091464	80 nM	1091364	9.1323E-05	0.007305173	$y = -0.0016x + 0.0002$	0.1250	75	625
	24	113268	10 nM	113244	0.000211932	0.002118869				
<i>P. p.</i> Chol. + ATPase	6397	6242524	500 nM	6236127	0.001025743	0.51237288				
	2171	1091464	80 nM	1089293	0.001992729	0.159125725	$y = -0.0034x + 0.0027$	0.7941	478	294.12
	313	113268	10 nM	112955	0.002768056	0.027633577				
<i>P. p.</i> S- α 3 β 1	1777	6242524	500 nM	6240747	0.000284795	0.142356948				
	692	1091464	80 nM	1090772	0.000634107	0.050696435	$y = -0.0057x + 0.0011$	0.1930	116	175.44
	124	113268	10 nM	113144	0.001092999	0.010918059				
SMD1168 + ATPase	1971	6242524	500 nM	6240553	0.000315891	0.157895535				
	658	1091464	80 nM	1090806	0.000603529	0.048253233	$y = -0.0052x + 0.0011$	0.2115	127	192.31
	135	113268	10 nM	113133	0.001193286	0.011918635				